UNDERSTANDING THE ROLE OF ACCESSORY PROTEINS ON ENAC FUNCTION

by

Daniel Horn, B.S.

A thesis submitted to the Graduate Council of
Texas State University in partial fulfillment
of the requirements for the degree of
Master of Science
with a Major in Biochemistry
December 2014

Committee Members:

Rachell Booth, Chair

Kevin Lewis

Wendi David

FAIR USE AND AUTHOR'S PERMISSION STATEMENT

Fair Use

Duplication Permission

ACKNOWLEDGEMENTS

Firstly, I would like to thank Dr. Rachell Booth for all of her help with this project. When I first joined the lab, I had no direction in life and had no idea what I was going to do with myself. Dr. Booth allowed me to join, however, and gave me a chance to do research which I didn't even know if I would like. Her constant support helped get me through the end of my undergraduate career and allowed me to flourish as a graduate student. In addition to Dr. Booth, I would also like to thank the members of my committee; Dr. L. Kevin Lewis and Dr. Wendi David, whose advice for my experiments were paramount to my success in graduate school.

Secondly, I would like to thank all of the members of the Booth research lab, past and present, who have helped me along the way especially Ty Whisenant, Samantha Swann, and Esther Lee. Ty got me interested in doing lab work and helped to train me in some of the techniques found in this document. Samantha always kept me cheerful and made the failures associated with research easier to deal with even at two o'clock in the morning. Without Esther keeping me grounded and also being extremely supportive, I would not have survived graduate school. There is not enough room to acknowledge everyone in the lab, but the other people I have worked with over the past three and a half years have also added to my success and their contribution to it should not be minimalized.

Last, but most certainly not least, I would like to thank my family. My parents,

Ken and Lynn, and my sister Trish have supported me throughout my college career until I finished which took a little longer than expected. Without the contributions of everyone mentioned, I would not be where I am today.

TABLE OF CONTENTS

Page

LIST OF FIGURES

Figure **Page**

ABSTRACT

The epithelial sodium channel (ENaC) reabsorbs sodium in the distal convoluted tubules of the nephron in kidneys. Regulation and assembly of ENaC is not well characterized and the use of a yeast deletion library can shed light on the matter. The gene for Wasabi (a form of enhanced green fluorescent protein) was fused to the 5' end of the gene for αENaC and then subcloned into the yeast expression vector pYES2/NTA. The vector with the new gene for Wasabi-αENaC was transformed into BY4742 yeast cells and into four single gene deletion mutants of yeast: *scj1, jem1, ypk1* and *lhs1*. Survival assays, western blots, and co-localization studies were used to verify expression of the Wasabi-tagged αENaC and monitor localization of the fusion protein inside *Saccharomyces cerevisae* yeast cells. We report that deletion of *SCJ1* did not affect ENaC function or localization, while deletions of *JEM1 and LHS1* appear critical for degradation of misfolded ENaC in the ER and the deletions lead to localization of ENaC in the ER. We also report that *YPK1* deletion prevented the yeast from expressing ENaC in the cell so localization and function could not be determined. Additional studies including cell surface biotinylation, co-immunoprecipitation, and additional confocal microscopy studies utilizing fluorophore-conjugated antibodies to illuminate cellular components (ER, Golgi, membrane, etc.) could be employed to further study localization.

CHAPTER I

Introduction and Literature Review

High Blood Pressure

High blood pressure, or hypertension, affects millions of Americans. According to the Centers for Disease Control (CDC), approximately 1 of every 3 adults in America (an estimated 67 million people) is affected by high blood pressure (1). High blood pressure also increases the risks for having other associated health problems such as heart disease or stroke. In addition to these increased risks, hypertension is also very costly to Americans. In 2011, costs associated with hypertension reached an estimated $51 billion with approximately $47.5 billion going towards direct medical costs stemming from having high blood pressure and linked health problems, and about $3.5 billion due to lost productivity at work (1). Sodium imbalance is one of the leading causes of hypertension, and the critical amount of sodium is reabsorbed into the blood stream in the kidney before excretion in urine. More specifically, this reabsorption occurs in the nephron of the kidney (FIG 1). Blood enters the nephron at the glomerulus where blood filtration occurs and the filtrate and blood cells are separated.

The blood is returned back to the cardiovascular system while the filtrate moves along through the proximal tubule and the loop of Henle where water reabsorption and sodium reabsorption occur to further concentrate the filtrate (FIG 1). Once the filtrate reaches the distal tubule of the nephron, the final 2-5% of sodium reabsorption occurs via the Epithelial Sodium Channel (ENaC) located in the distal convoluted tubule of the

nephron (2, 3). This reabsorption, the last before excretion as urine, is the most important for maintaining homeostasis of sodium and fluid balance in the body (4, 5).

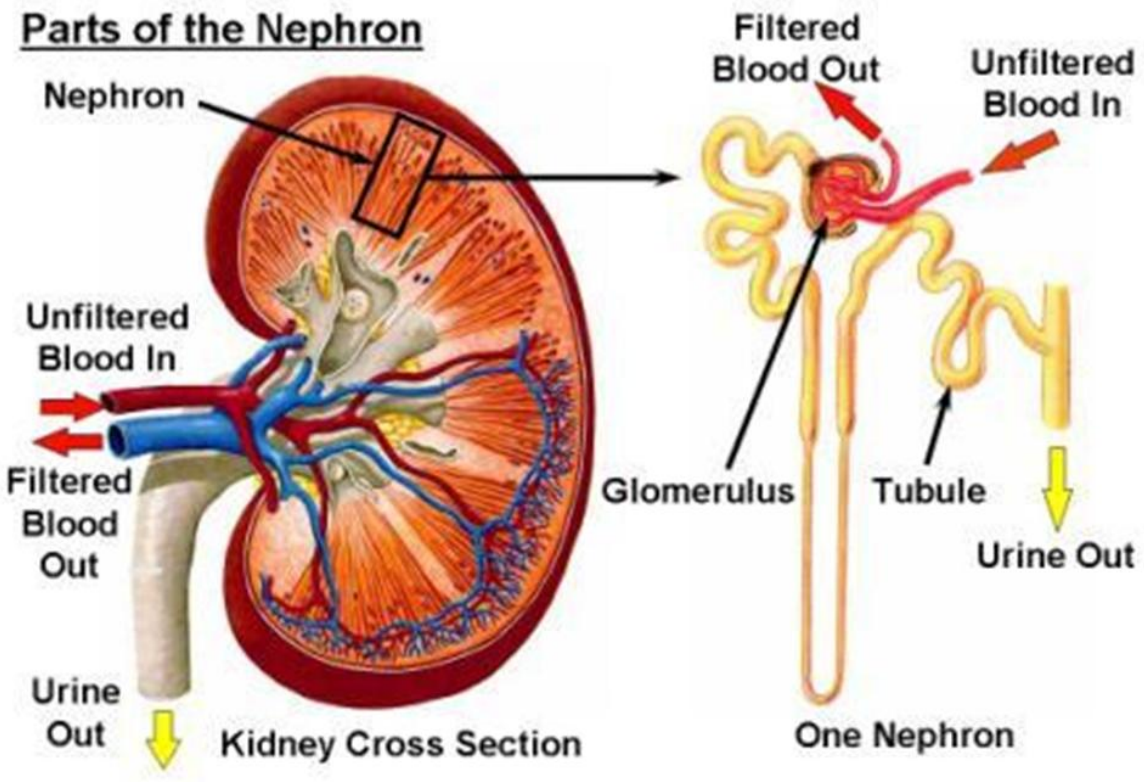

Guyton, Arthur C.; Hall, John E. (2006). *Textbook of Medical Physiology*. Philadelphia: Elsevier Saunders. pp. 310. ISBN 0-7216-0240-1.

FIG 1. Transverse cross-section of the kidney highlighting the nephron. Sodium reabsorption through ENaC occurs in the distal convoluted tubule of the nephron (the functional unit of the kidney) before the remaining filtrate is excreted as urine. There are approximately 1 million nephrons in each kidney

Epithelial Sodium Channel (ENaC) Features

ENaC is rate limiting for the reabsorption of sodium ions across the apical membrane of epithelial cells lining the distal convoluted tubule of the nephron (6). It is composed of three homologous, but distinct subunits (α, β and γ) which are brought together in a 1:1:1 stoichiometry (3-4, 6-9). ENaC shows activity with different compositions of α, β, and γ as long as the α-subunit is present because it is essential for

activity of the channel (3). The β and γ subunits are important for regulation of ENaC so even though the channel can function without them, they show the best channel activity when present (3). The channel pore is blocked by amiloride which is a diuretic that causes the excess salt and water to be excreted rather than being reabsorbed back into the bloodstream.

Each subunit of ENaC consists of two transmembrane domains with small N- and C-termini tails in the cytoplasm and a large extracellular loop (3). The C-terminus contains a PY motif [motif consisting of highly conserved proline and tyrosine residues with any two amino acids in between (PPXY in the case of ENaC)] which is critical for regulation of the channel (9-10). ENaC is non-ligand gated meaning that it does not require ligand binding for the channel to become active. The channel is constitutively active and forms a pore that remains open, but since it is highly selective for sodium due to the coordination of basic residues situated in the pore, it does not allow other non-specific compounds or ions to pass through the channel with the exception of small lithium cations (3). The hydrophobic transmembrane helices embed into the membrane like anchors for the large extracellular loop. The large extracellular loop comprises the largest portion of the protein and is responsible for formation of the central pore and interaction with the extracellular environment (9).

ENaC is situated on the apical membrane (FIG 2) of the epithelial cells, the side that the urine passes, alongside aquaporin channels that reabsorb water with sodium ions to maintain the concentration in the cell (3-4). A sodium-potassium-ATPase pump, found along the basolateral membrane, is responsible for pumping the sodium ions back

into the bloodstream while pulling potassium into the epithelial cell to be removed from the body through the urine (4).

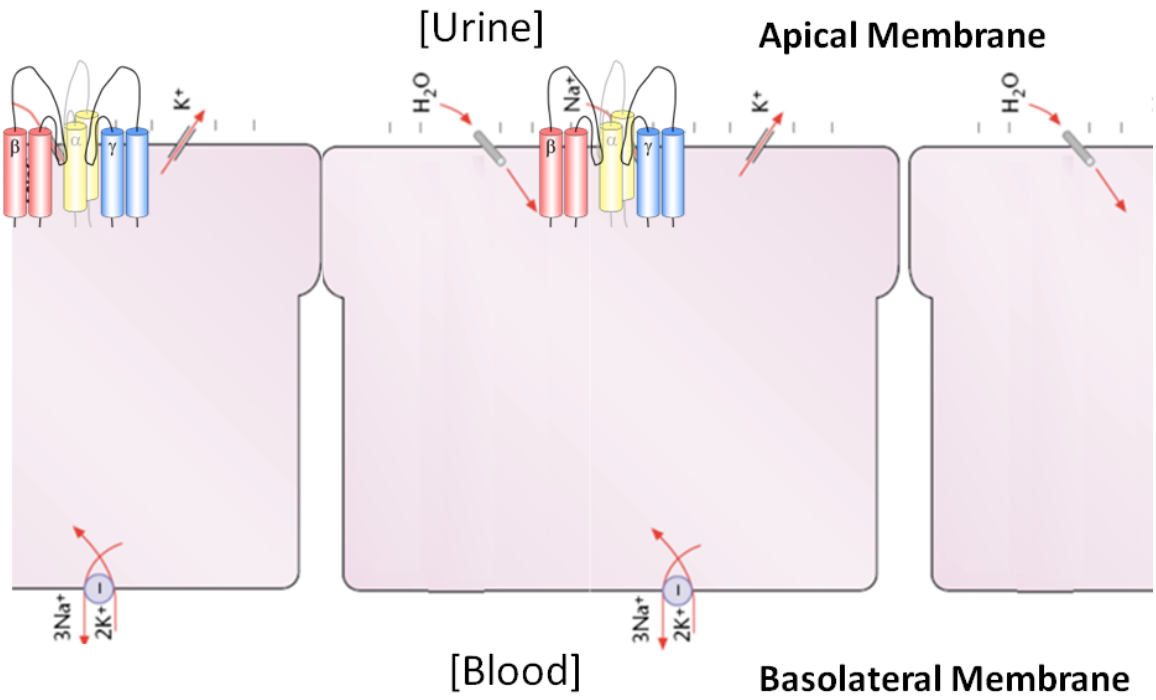

FIG 2. Representation of epithelial cells lining the distal convoluted tubules indicating sodium and potassium ion flow through the cells. Sodium enters the epithelial cells via ENaC found on the apical membrane of the epithelial cells. Water is reabsorbed through aquaporins along with ENaC to maintain the osmotic pressure in the cell. Sodium is then pumped into the blood stream through a Na^+/K^+-ATPase channel which brings potassium into the epithelial cells for excretion into the urine.

Although ENaC has not been crystallized, the proposed structure of ENaC (FIG 3) mentioned above was established by Dr. Stockand and colleagues at the University of Texas San Antonio Health Science Center along with Dr. Rachell Booth from Texas State University in 2008 (9). The projected structure was proposed due to the crystallization of another ion channel from the same superfamily, the acid-sensing ion channel (ASIC), which was crystallized the previous year in 2007 by Jasti and associates from the Howard Hughes Medical Institute and Cold Spring Harbor Laboratory (10). The two ion channels are in the same ENaC/Degenerin superfamily of proteins and have a lot of

shared structural features between them which allowed for the proposal of the ENaC structure even though the actual crystal structure has not been established yet (9). Alterations or mutations in this structure can lead to two genetic disorders relating to ENaC function.

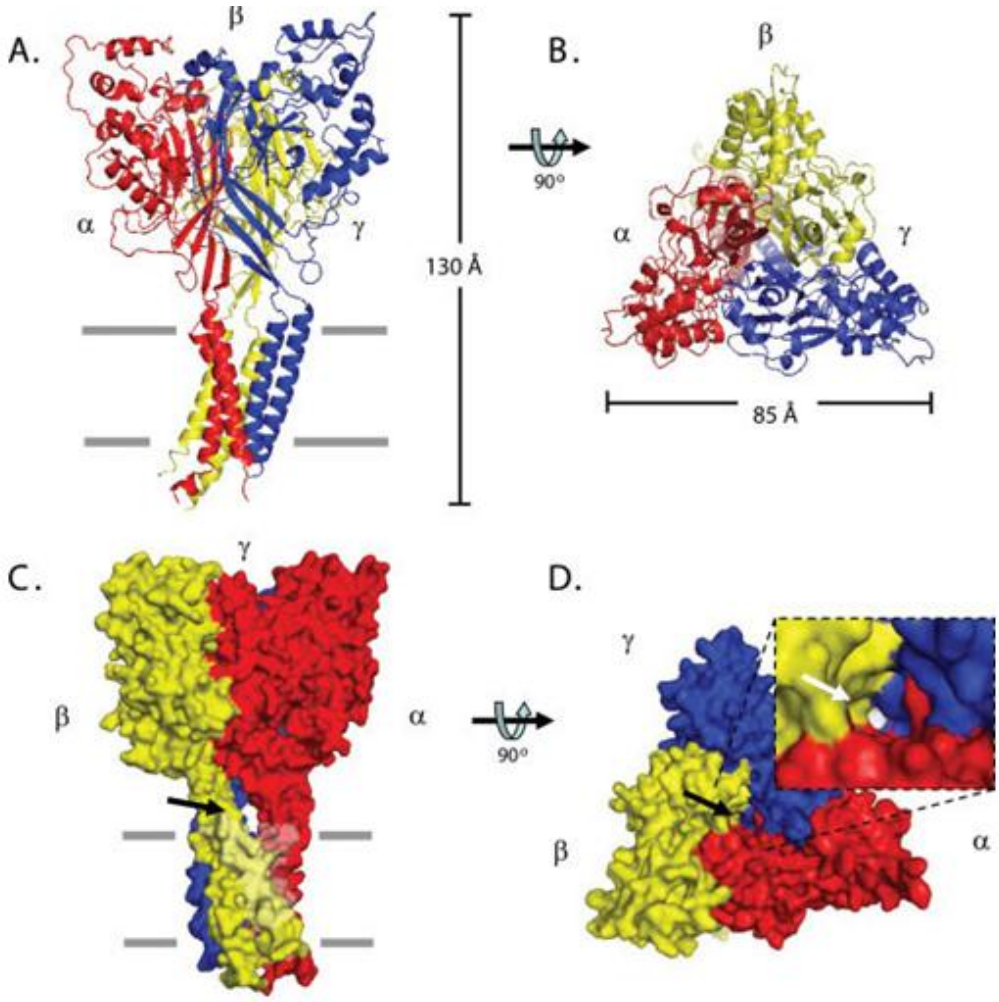

Reference: Stockand, J. D., *et al.* (2008) *IUBMB Life* **60**, 620-628

FIG 3. Proposed structure of ENaC. A and B are ribbon diagrams of the proposed structure of ENaC showing the side view (A) and top view (B) of the channel. C and D are space filling models of ENaC from the side (C) and top view (D). Arrows show the predicted pore location in ENaC.

ENaC Diseases

Genetic mutations to ENaC cause two diseases that have been very well

characterized, Liddle's syndrome and Pseudohypoaldosteronism type 1 (PHA 1). Liddle's syndrome is a genetic disorder caused by gain of function mutations to the α, β or γ subunits of ENaC (3, 8, 11-13). The mutation is a deletion of 45-75 amino acids from the C-terminus of the α, β or γ subunits of ENaC which removes the PY motif essential for the regulation of ENaC. This deletion leads to localization of ENaC in the membrane and hyperactivity of the channel which causes more sodium to be reabsorbed through the constitutively active channels which, in turn, leads to hypertension (3, 8, 11). In addition to the influx of sodium ions passing through the sodium-potassium-ATPase channel, a decrease in potassium levels in the blood is seen. Low potassium levels, also referred to as hypokalemia, can lead to other health effects (3).

The other disease, PHA-1, occurs when a frameshift or missense mutation affects α, β or γ subunits which causes loss of function in ENaC. The loss of function prevents reabsorption of sodium leading to low blood pressure, hypotension, and dehydration since less water is being reabsorbed through the aquaporins (3, 8, 11). Hyperkalemia, or high potassium levels, is also seen due to the lack of reabsorption of sodium which cannot then stimulate the removal of potassium from the blood because of the reduced function of the sodium-potassium-ATPase channel on the basolateral membrane of the epithelial cells (8, 11). In addition to blood pressure disorders caused by mutations, ENaC is also regulated through hormones, proteins and other peptides.

Regulation of ENaC

The regulation of ENaC can occur through upregulation due to hormones and

down regulation through Nedd4. The first hormone to look at is aldosterone. Aldosterone regulation works by first activating the kinase SGK 1. Once activated, SGK1 can directly activate ENaC, though that mechanism isn't well understood, or it can phosphorylate Nedd4 which induces binding of the protein 14-3-3 (FIG 4) and prevents the interaction of Nedd4 and ENaC (3-4). Aldosterone is also seen to deubiquitinate another enzyme, Usp2-45, which leads to an increase in ENaC activity (3). To summarize, aldosterone upregulation leads to increased ENaC expression in the membrane, activity, and therefore, increased blood pressure.

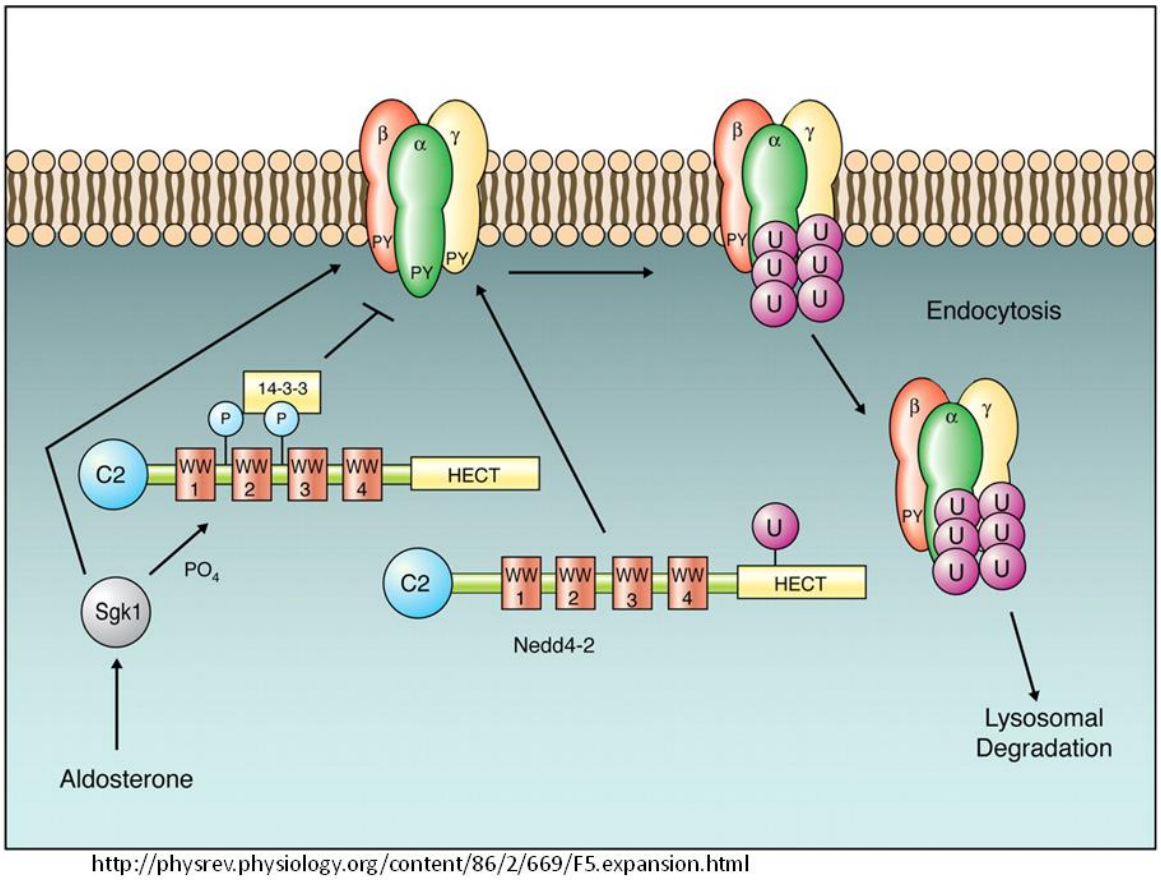

http://physrev.physiology.org/content/86/2/669/F5.expansion.html

FIG 4. Aldosterone and Nedd4 regulation of ENaC. Aldosterone activates SGK1 which phosphorylates Nedd4-2 which recruits the protein 14-3-3 to Nedd4-2, and then prevents the interaction of the WW domains of Nedd4-2 with the PY motif of ENaC. This phosphorylation prevents the transfer of ubiquitin to ENaC and stops lysosomal degradation. SGK1 can also interact with ENaC, directly upregulating expression of ENaC in the membrane though the mechanism for this is not well known.

Another hormone, vasopressin, is also important in the regulation of ENaC. Vasopressin binds to receptors called V2 receptors, releasing cAMP, causing the number of ENaC channels in the membrane to increase (3). This causes high blood pressure because of the increase in ENaC expression at the membrane and the increase in sodium reabsorption. Studies indicate that vasopressin, like aldosterone, stimulates a kinase called PKA which also phosphorylates Nedd4 to block ENaC degradation after PKA is stimulated by increased cAMP levels in the cell (14). Aldosterone and vasopressin increase the activity of ENaC while Nedd4 decreases the activity of ENaC.

Nedd4 is an E3 ubiquitin ligase that contains 3-4 WW domains and a HECT domain (3, 10). The WW domains consist of 2 highly conserved tryptophan residues separated by 20-22 amino acids. This domain interacts with the PY motif of ENaC on the α, β or γ subunits (3, 10). The HECT domain of Nedd4 is a ubiquitin transferase domain which, when in close enough proximity to ENaC due to the interaction of the WW domain and PY motif, transfers ubiquitin from Nedd4 to ENaC (3-4, 10). Ubiquitin is a small protein that signals the cell to degrade the protein to which it is bound. Once ENaC is tagged with ubiquitin, it is pulled back into the cell via clathrin-mediated endocytosis and sent to the lysosome to be degraded. (4) Since Nedd4 needs the interaction with the PY motif to ubiquitinate ENaC, it is believed that Liddle's Syndrome occurs because of Nedd4's inability to bind with ENaC because of the deletion of the PY motif causing overexpression of ENaC. (10)

Goal

In addition to Nedd4, PKA and SGK1, other proteins are believed to potentially affect ENaC maturation or function. In order for ENaC to mature and get from the endoplasmic reticulum to being fully functional at the plasma membrane, ENaC requires assistance from accessory proteins to help it fold properly, traffic around the cell, insert into the membrane or to be activated. An initial search of the literature found several proteins thought to affect maturation. To study which of the proteins affected ENaC, a yeast deletion library was utilized containing single deletions of genes coding for these proteins which could give insight to how the proteins function with respect to ENaC. This study focused on 4 of those proteins: Scj1, Jem1, Ypk1, and Lhs1.

Scj1 and Jem1 are heat shock proteins with molecular weights of approximately 40 kDa (also known as Hsp40 chaperones). Scj1 and Jem1 are found in the ER and are the yeast homologs of DnaJ proteins found in *E.* coli and function to help translocate and fold proteins in the ER (15). More specifically, in yeast these two proteins were found to be a part of the ER associated degradation (ERAD) pathway and help remove misfolded proteins from the ER to be degraded in the cytosol (15). Ypk1 is the yeast homolog of the mammalian protein Sgk1 which, as mentioned above, phosphorylates Nedd4 and prevents ubiquitination of ENaC in the plasma membrane. Ypk1 has also been shown to help maintain the integrity of the cell wall in yeast (16). Lhs1 is a heat shock protein, MW 70 kDa, (Hsp70) that helps translocate and fold proteins found in the ER and was also found to be part of the ERAD (17).

The goal of this project was to identify and understand the roles of these

additional accessory proteins and how they affect the localization, trafficking, folding, or function of ENaC. The studies employed using fluorescently tagged ENaC to monitor growth of the yeast as well as protein localization and expression of ENaC within deletion strains. The studies presented here could allow researchers the ability to elucidate a folding and maturation pathway for ENaC by monitoring its function as genes for accessory proteins are deleted and allow our lab to screen other accessory protein candidates available in the deletion library.

CHAPTER II

Materials and Methods

Cloning Wasabi-αENaC for Yeast Expression

All polymerase chain reaction (PCR) and cloning buffers, enzymes and NEB 5-alpha competent *E. coli* cells were purchased from New England Biolabs (Ipswich, MA) unless noted otherwise. Plasmid DNA, pmWasabi-αENaC, was received as a generous gift from Dr. Jim Stockand (UTHSCSA, San Antonio, TX) and contained the gene for the enhanced green fluorescent protein (EGFP) called Wasabi (developed by Allele Biotechnology in San Diego, CA) fused to the gene for the mouse α-subunit of ENaC (αENaC). Primers for PCR were designed against the genes and synthesized by Integrated DNA Technologies (Coralville, IA). Primers are listed in the table below (Table 1). EcoRI and NotI restriction sites were engineered on the ends of the primers so the genes could be subcloned into matching sites in the yeast expression vector, pYES2/NTA which was purchased from Life Technologies (Carlsbad, CA). PCR was carried out using 100 ng pmWasabi-αENaC template DNA, 0.5 µM forward and reverse primer (listed in Table 1), 200 µM dNTPs, 1X Q5 Reaction Buffer, and 2 units Q5 High-Fidelity DNA polymerase in a total reaction volume of 50 µL. PCR was started at 98 °C for 10 s, and then 35 cycles were run at 98 °C for 10 s, 59 °C for 30 s and 72 °C for 2 min with one last extension after the final cycle at 72 °C for 2 min. The PCR product was analyzed using agarose gel electrophoresis to verify amplification of the genes.

Table 1: Primers used in PCR.

Primer Name	Primer Sequence
Wasabi/EYFP Forward (EcoRI)	5'-GCAAGAATTCTTATGGTGAGCAAGGGCGAGGAGC-3'
αENaC Reverse (NotI)	5'-GCAAGCGGGCCTCAGAGTGCCATGGCCGGAGC-3'

The PCR product (Wasabi-αENaC) was cleaned and concentrated using the DNA Clean & Concentrator™-5 kit from Zymo Research (Irvine, CA) and following the prescribed protocol from the kit. Restriction digests were then completed to create compatible sticky ends on the pYES2/NTA vector and Wasabi-αENaC PCR product for ligation together. Each digestion reaction (vector and PCR product) contained 1 X NEBuffer EcoRI, DNA (cleaned and concentrated Wasabi-αENaC PCR product or 2.5 µg pYES2/NTA plasmid DNA), 20 units of EcoRI and 10 units of NotI in a total reaction volume of 50 µL. The digestion reactions were incubated for 1 hour at 37 °C before heat inactivation of the enzymes at 65 °C for 20 min. Reactions were loaded into a 0.7 % TAE agarose (w/v) gel with loading dye at a 1X concentration and electrophoresis was run for 1 hour at 130 volts to resolve the fragments of DNA. This DNA was to be excised from the gel and cleaned for ligation of the Wasabi-αENaC gene into pYES2/NTA vector.

Gel extraction was performed using the QIAEX II Gel Extraction kit and supplied protocol from Qiagen (Venlo, Netherlands). The DNA samples were quantitated to check yields and purity using the NanoDrop 2000 UV/Vis Spectrophotometer from Thermo Fisher Scientific (Waltham, MA). The insert and vector were ligated together in a 3:1

molar ratio (150 ng insert: 100 ng vector) with 1X T4 DNA Ligase Buffer and 400 units of T4 DNA Ligase in a 20 µL reaction. A vector only negative control was also prepared. For both the ligation reaction and the vector only negative control, 5 µL of each reaction mixture was transformed into NEB 5-alpha competent *E. coli* cells using the High Efficiency Transformation Protocol from New England Biolabs and the *E. coli* was grown on LB plus ampicillin plates overnight at 37 °C. Four clones were picked from the plate and grown overnight while shaking at 37 °C in LB broth plus ampicillin. The plasmid DNA was isolated from the clones using the QIAprep Spin Miniprep Kit from Qiagen and the accompanying protocol with the exception of eluting the DNA from the spin column using water instead of the included elution buffer. DNA from one of the clones was sequenced by Quintara Biosciences (Albany, CA) to verify ligation of the insert to the vector. This was verified by aligning the sequencing data with the genes for Wasabi and αENaC using the Clustal Omega program from the European Bioinformatics Institute website.

In addition to sequencing, restriction digests were done on the pYES2/NTA/Wasabi-αENaC DNA using ApaI and XhoI single digestions as determined by a sequence map that was created based on the predicted sequence of pYES2/NTA/Wasabi-αENaC. The digestion of 1 µg of pYES2/NTA/Wasabi-αENaC DNA was carried out in 1X Cutsmart™ buffer from New England Biolabs with 50 units of ApaI in a total reaction volume of 50 µL. The reaction was incubated for 1 hour at 25 °C and then heat inactivated for 20 minutes at 65 °C. Digestion of 1 µg of pYES2/NTA/Wasabi-αENaC with XhoI was done in 1X Cutsmart™ buffer with 20 units of XhoI in a total

reaction volume of 50 µL. The digestion was incubated at 37 °C and then heat inactivated for 20 minutes at 65 °C. After heat inactivation, loading dye was added to the reactions at a concentration of 1X and 5 µL of each reaction was subjected to agarose gel electrophoresis to analyze the fragments of DNA produced by digestion.

Expression in Yeast

The resulting plasmid, pYES2/NTA/Wasabi-αENaC, was transformed into BY4742 yeast cells as well as 4 yeast deletion strains (*scj1, jem1, ypk1* and *lhs1*), generously donated by Dr. Kevin Lewis at Texas State University and originally purchased from Open Biosystems (now GE Healthcare, Little Chalfont, United Kingdom), using the following high efficiency lithium acetate transformation protocol. Overnight cultures of yeast were grown shaking at 30 °C in YPDA (1% yeast extract, 2% peptone, 2% glucose, and 0.002% adenine) and diluted the following day to an OD_{600} of 0.1. Cultures were grown until an OD_{600} of 0.4-0.7 was obtained. One mL of cells were pelleted by centrifugation at max speed for 30 seconds and the supernatant was discarded. To the pellet, the following reagents were added in order; 240 µL PEG 3350 (Mallinckrodt, St. Louis, MO), 36 µL 1 M lithium acetate (Sigma-Aldrich, St. Louis, MO), 10 µL sonicated salmon sperm DNA (Agilent Technologies, Santa Clara, CA), 2.5 µL β-mercaptoethanol (G Biosciences, St. Louis, MO), 1.5 µg plasmid DNA and ddH_2O to a final volume of 360 µL of liquid with the pellet. Cells were vortexed for one minute and then incubated at 42 °C for 20 minutes. Cells were centrifuged for 2 min at 2000 x g, the supernatant was discarded and the cells were resuspended in 200 uL ddH_2O. The cells were then spread

on SC-Uracil agar plates containing 2% glucose and incubated at 30 °C for 2 days until individual colonies grew.

Single colonies of each transformant were picked and grown in 15 mL SC-uracil containing 2% glucose overnight at 30 °C while shaking. The OD_{600} was measured the following morning, and once the amount of overnight culture needed to obtain an OD_{600} = 0.4 in 50 mL of induction media (SC-uracil containing 2% galactose) was determined; the cells were centrifuged for 5 min at 1500 x g. The pellet was resuspended in 50 mL induction media and grown for 8 hours shaking at 30 °C. Whole cell lysates were made using the post alkaline extraction method as described by Vitaly Kushnirov in 2000 (18). The lysates were analyzed via SDS-PAGE using a 4% stacking and 7.5% resolving gel. The protein was transferred to a nitrocellulose membrane for western blotting using the Trans-Blot® Turbo™ Transfer System from Bio-Rad (Hercules, CA). The membrane was first probed with the Anti-Xpress™ antibody (Life Technologies) using a dilution of 1:5000 in blocking solution (1X TBS, 0.1% v/v Tween 20, and 5% w/v dry milk). Western Lightning Plus ECL (Perkin Elmer, Waltham, MA) chemiluminescence substrate was used to detect the Wasabi-αENaC fusion protein and imaged using the ChemiDoc™ XRS+ System from Bio-Rad Laboratories. The membrane was stripped of antibodies using the mild stripping buffer (1.5% w/v glycine, 0.1% w/v SDS, and 1% Tween20 pH 2.2) and protocol from Abcam (Cambridge, England) and probed again with an Anti-αENaC antibody from StressMarq Biosciences (Victoria, BC) at a 1:1000 dilution in blocking solution to verify the presence of ENaC. The membrane was stripped again of antibodies and probed for a third time with an Anti-β-actin antibody from Santa Cruz Biotechnology

(Dallas, TX) at a 1:1000 dilution in blocking solution.

Survival Dilution Growth "Pronging" Assay

BY4742 cells along with the four yeast deletion strains were transformed with pYES2/NTA and pYES2/NTA/Wasabi-αENaC (same transformants from expression study) and grown on SC-uracil containing 2% glucose. Yeast cells were harvested in water and diluted 1/40. They were then subjected to sonication for 8 seconds and the cells counted using a hemacytometer and microscope. Cells (2×10^7) were added to a 96-well plate and diluted 5-fold across 6 wells. The dilutions were pronged onto selective plates and incubated at 30 °C for 5 days. Selective plates contained 2% galactose with additional salt at a concentration of 0.75 M to show differences in growth and to determine functionality of Wasabi-αENaC.

Confocal Microscopy and Localization Studies

Cells were prepared by inducing expression of Wasabi-αENaC in 10 mL SC-Uracil liquid media with 2% galactose. The cells were pelleted, washed twice with PBS, and resuspended in PBS with formaldehyde at a 4% v/v concentration to fix them. The cells were then washed twice with PBS and then wet mounted to microscope slides. The cover slip was affixed to the slide with acrylic. Imaging was conducted using the Olympus FLUOVIEW FV1000 confocal laser scanning microscope with a 60X oil immersion lens and accompanying software. Wasabi fluoresced after excitation with a laser producing light at a wavelength of 405 nm.

Cell localization studies were carried out by preparing cells the same way. The final resuspension was done in a solution of 1X Hoechst 33342 (diluted from a 10,000X concentrate) in PBS and incubated for 20 minutes. After incubation the cells were wet mounted as before and imaged using the confocal microscope. The Hoechst 33342 dye (after intercalation into the nuclear DNA) fluoresced after excitation with light at 350 nm.

CHAPTER III

Results and Discussion

To investigate the role that potential accessory proteins play on ENaC maturation and function, localization studies were performed on yeast to monitor how deletion of genes coding for those potential accessory proteins affected the distribution of ENaC within the cell. This information could be used to elucidate the roles that accessory proteins have on the folding, function or trafficking and insertion of ENaC into the plasma membrane. In these studies, the gene for a green fluorescent protein (Wasabi) that was fused to the 5' end of the gene for αENaC was subcloned into a yeast expression vector and expressed in yeast. With this, growth assays and localization studies performed on yeast deletion strains were used to determine localization of the Wasabi-αENaC when deletion of genes occurs.

Cloning Wasabi-αENaC for Yeast Expression

Wasabi-αENaC fused genes were amplified via PCR from pmWasabi-αENaC (donated by the Stockand lab, UTHSCSA) PCR products were approximately 3 kb in size and the control reaction with no template DNA yielded no PCR product (FIG 5). The gene for αENaC from *Mus musculus* is 2238 bp (19) and the gene for Wasabi is 711 bp (20) which, when fused together, give the apparent 2.9 kb fragment seen via gel electrophoresis (FIG 5).

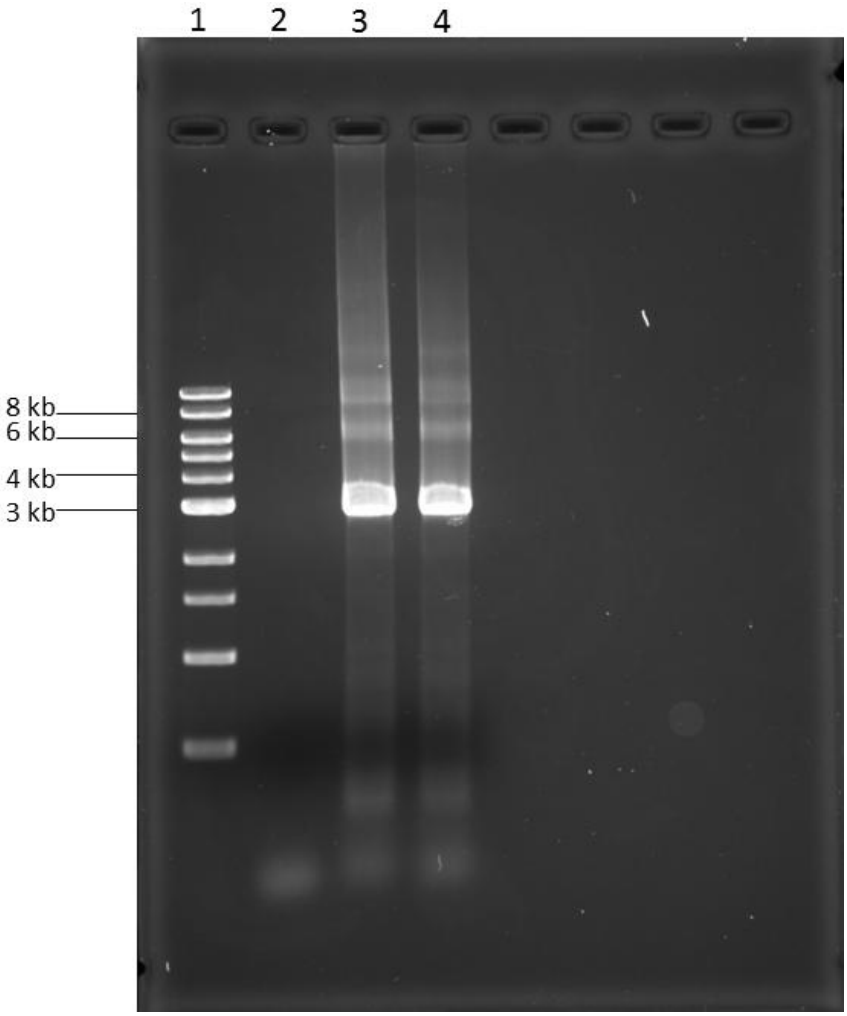

FIG 5. **Polymerase Chain Reaction (PCR) amplification of Wasabi-αENaC genes from pmWasabi-αENaC plasmid DNA.** The genes were amplified and run on a 0.8% w/v agarose gel to verify reactions. *lane 1,* 1 kb DNA ladder. *lane 2,* negative control with no pmWasabi-αENaC template DNA. *lane 3,* Wasabi-αENaC amplification. *lane 4,* Wasabi-αENaC duplicate. Stained with ethidium bromide.

The Wasabi-αENaC PCR product and a yeast expression plasmid, pYES2/NTA/αENaC, were each digested with the restriction enzymes EcoRI and NotI. This digestion was performed to remove the αENaC gene from pYES2/NTA (i.e., empty vector) and to create compatible sticky ends on the Wasabi-αENaC PCR product for cloning into the multiple cloning site (MCS) of pYES2/NTA. The digestion products were separated on a 0.7% TAE agarose (w/v) gel to determine size and appropriate DNA

fragments were excised from the gel (FIG 6). The 3 kb Wasabi-αENaC PCR product was extracted as well as the 6 kb fragments for pYES2/NTA (FIG 6, lanes 3-4 and 6-7, respectively).

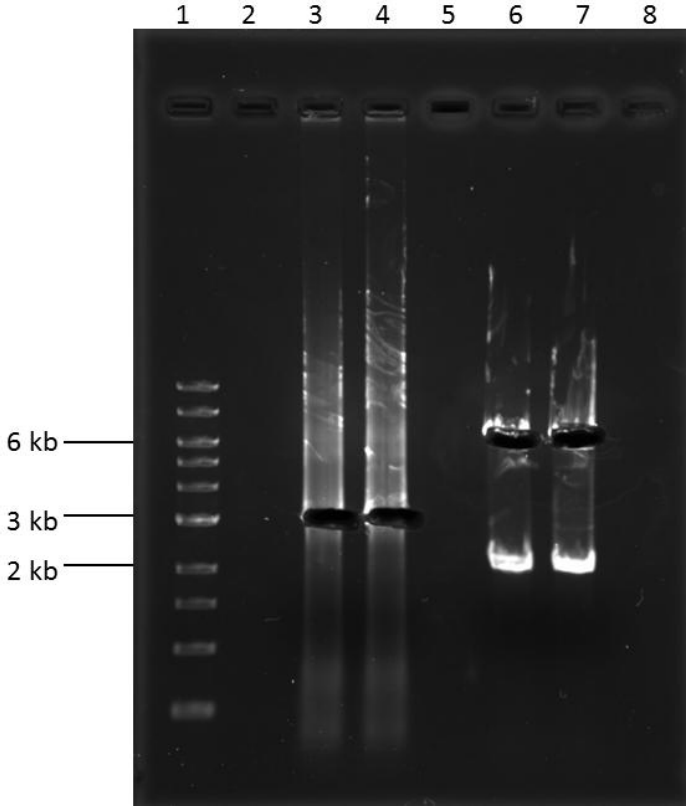

FIG 6. **Gel extraction of digested Wasabi-αENaC pcr product and digested pYES2/NTA plasmid DNA.** Digested Wasabi-αENaC PCR product and digested pYES2/NTA/αENaC were separated on a 0.7% agarose gel and gel extracted using the Qiagen QIAEX II Gel Extraction Kit. *lane 1*, 1 kb DNA ladder. *lane 2,* empty. *lanes 3-4*, Wasabi-αENaC PCR product after EcoRI and NotI digestion (duplicate). *lane 5,* empty. *lanes 6-7*, digested pYES2/NTA/αENaC (duplicate). Stained with ethidium bromide.

The empty pYES2/NTA vector is 6021 bp (21) and migrated to the same position as the 6 kb fragment in the 1 kb DNA ladder. After gel extraction, the Wasabi-PCR product and empty pYES2/NTA were cleaned up with the Qiagen QIAEX II Gel Extraction Kit (FIG 6) and quantitated using the NanoDrop 2000 UV/Vis Spectrophotometer (Thermo Fisher Scientific). These DNA fragments were ligated together in a 3:1 molar ratio of PCR product to empty vector DNA (equivalent to 150 ng PCR product and 100 ng

empty vector) for 10 minutes at room temperature using T4 DNA ligase (New England Biolabs) in 1X T4 DNA ligase buffer. After 10 minutes, the ligation reaction mixture was transformed into NEB 5-alpha competent *E. coli* using the High Efficiency Transformation Protocol from New England Biolabs, plated on LB plus ampicillin plates to select for transformants expressing ampicillin resistance, and grown overnight at 37 °C.

After ligation of the Wasabi-αENaC PCR product into the pYES2/NTA vector and transformation into 5-alpha *E. coli*, the pYES2/NTA/Wasabi-αENaC plasmid DNA was isolated from a culture of bacteria using the QIAprep Spin Miniprep Kit from Qiagen. Resulting plasmid clones were analyzed on a 1% w/v TAE agarose gel (FIG 8). The uncut pYES2/NTA plasmid (6 kb empty vector) migrated to approximately 4.5 kb when compared to the 1 kb DNA ladder while pYES2/NTA/αENaC (~8.2 kb) migrated to approximately 6 kb (FIG 7, lanes 2 and 3, respectively). The pYES2/NTA/Wasabi-αENaC (8970 bp) from each of the 4 clones ran at approximately 6.5 kb which, when supercoiled, would explain the difference in migration between it and the pYES2/NTA/αENaC (FIG 7).

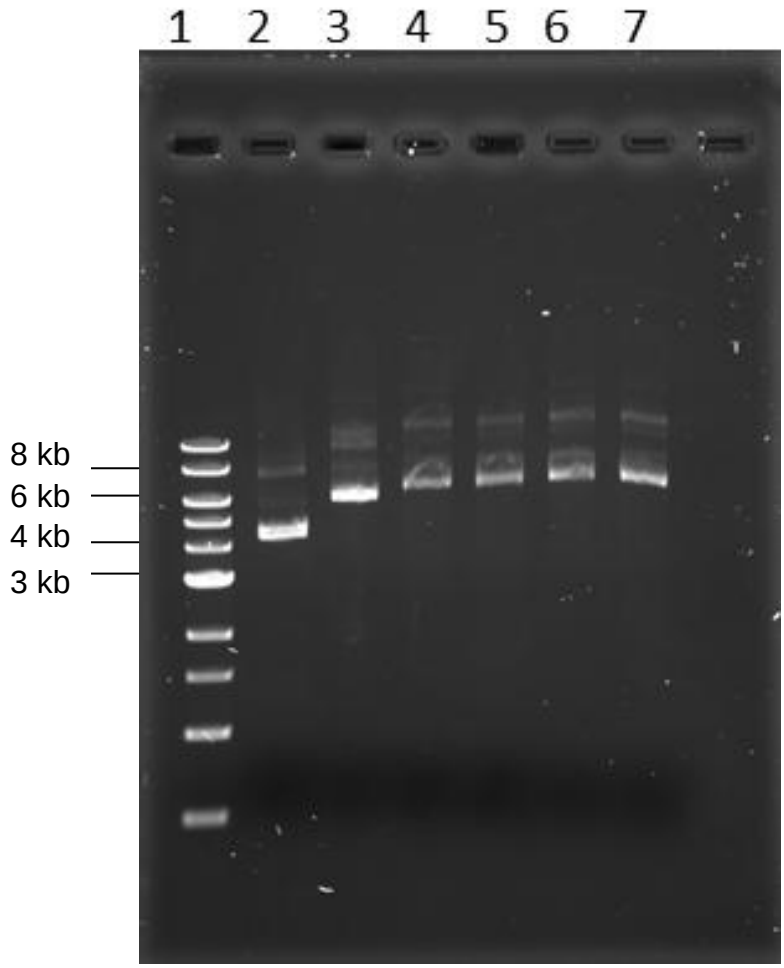

FIG 7. **pYES2/NTA/Wasabi-αENaC plasmid isolation from 5-alpha competent cells.** The ligation reaction was transformed into 5-alpha competent cells and plasmid DNA was isolated from 4 transformant colonies before sequencing. *lane 1,* 1 kb DNA ladder. *lane 2,* pYES2/NTA empty vector. *lane 3,* pYES2/NTA/αENaC. *lanes 4-7,* pYES2/NTA/Wasabi-αENaC plasmid DNA from clones 1-4. Stained with ethidium bromide.

To help determine that Wasabi-αENaC was properly cloned, a restriction map for pYES2/NTA/Wasabi-αENaC was created (the sequence was about 8.97 kb long) and analyzed using the NEBcutter® program on the New England Biolabs website. The restriction enzymes ApaI and XhoI were predicted to cut pYES2/NTA/Wasabi-αENaC creating fragments of ~4.2 kb, 2.8 kb, and 1.9 kb with ApaI alone and fragments of ~6.8 kb and 2.1 kb with XhoI alone. Single digestions of the pYES2/NTA/Wasabi-αENaC clone #1 (FIG 8, lane 4) were performed in addition to double digestion reactions of

pYES2/NTA/Wasabi-αENaC and pYES2/NTA/αENaC with EcoRI and NotI to remove the Wasabi-αENaC and αENaC genes, respectively. Digestion products were analyzed in a 1% w/v TAE agarose gel. Digestion of pYES2/NTA/αENaC with EcoRI and NotI gave DNA fragments of approximately 6 kb and 2.2 kb indicating the EcoRI and NotI restriction enzymes were able to remove the αENaC gene (FIG 8, lane 4). Wasabi-αENaC was cut from pYES2/NTA/Wasabi-αENaC plasmid using EcoRI and NotI and yielded DNA fragments of approximately 6 kb and just below 3 kb in size (FIG 8, lane 7) which corresponds to the removal of αENaC from pYES2/NTA (FIG 8, lane 4) except that the gene for Wasabi is fused to αENaC accounting for the difference in size from 2.2 kb to ~3 kb. The ApaI and XhoI single digests of pYES2/NTA/Wasabi-αENaC, when run on the gel, gave fragments of DNA at 4.2 kb, 2.8 kb and 1.9 kb and fragments of 6.8 kb and 2.1 kb in size, respectively (FIG 8). These results matched the predicted results from the NEBcutter® program as well as results from the initial cloning of pYES2/NTA/αENaC (22). The pYES2/NTA/Wasabi-αENaC plasmid was then sent to Quintara Biosciences for sequencing. Sequence alignments, using the Clustal Omega program available from the European Bioinformatics Institute website, were used to check for errors in the Wasabi and αENaC genes.

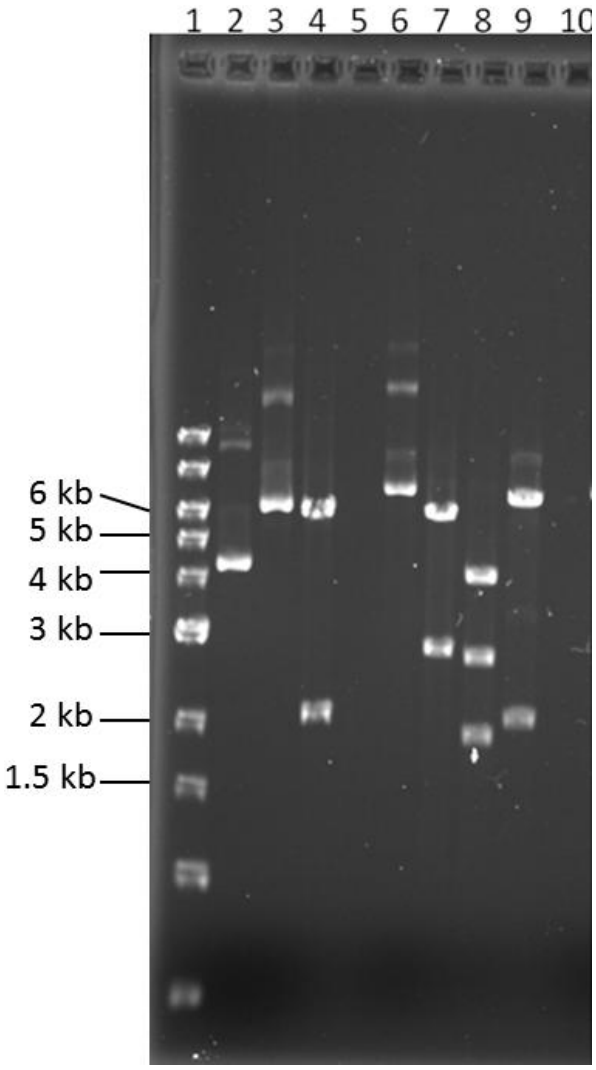

FIG 8. **Restriction enzyme digestion of pYES2/NTA/Wasabi-αENaC to verify cloning.** pYES2/NTA/αENaC and pYES2/NTA/Wasabi-αENaC plasmids were digested with restriction enzymes and run on a 1% agarose gel. *lane 1,* 1 kb DNA ladder. *lane 2,* uncut pYES2/NTA plasmid DNA. *lane 3*, uncut pYES2/NTA/αENaC. *lane 4,* EcoRI and NotI double digestion of pYES2/NTA/αENaC. *lane 5,* empty. *lane 6,* uncut pYES2/NTA/Wasabi-αENaC . *lane 7,* EcoRI and NotI double digestion of pYES2/NTA/Wasabi-αENaC. *lane 8,* ApaI digestion of pYES2/NTA/Wasabi-αENaC. *lane 9*, XhoI digestion of pYES2/NTA/Wasabi-αENaC. Stained with ethidium bromide.

Expression of Wasabi-αENaC in Yeast

The plasmids pYES2/NTA/αENaC, pYES2/NTA/Wasabi-αENaC, and pYES2/NTA/LacZ were transformed into yeast (pYES2/NTA/αENaC and pYES2/NTA/LacZ transformed into BY4742 cells only) using the high efficiency lithium acetate transformation protocol detailed above. Colonies were patched onto SC-Uracil plates with 2% glucose and the colonies used for these expression studies were the same

colonies used in the pronging assay. Cultures were grown overnight in SC-Uracil with 2% glucose and cells were resuspended in SC-Uracil with 2% galactose and grown for 8 hours shaking at 30 °C to induce expression. Cells were lysed using the post-alkaline extraction method as outlined earlier. Whole cell lysates were subjected to SDS-PAGE for western blotting.

Western blotting was used to verify expression of the Wasabi-αENaC fusion protein in the control yeast strain of BY4742 as well as the strains containing deletions of *SCJ1, JEM1, YPK1,* and *LHS1*. In addition, and for comparison, pYES2/NTA/LacZ plasmid and pYES2/NTA-αENaC plasmid were transformed into BY4742 cells. LacZ is a gene encoding a ~120 kDa protein called beta-galactosidase and was used as a positive control for the Anti-Xpress™ antibody (FIG 9). Alpha ENaC's approximate MW is 78 kDa, but it has been shown that glycosylation patterns can add an additional 15-20 kDa to the apparent MW, which was seen when the protein migrated to approximately 100 kDa (FIG 9). Wasabi fused to αENaC adds an additional 30 kDa to the MW of αENaC that can be seen in the BY4742 control and the 3 deletion strains in lanes 4-7 (FIG 9). αENaC expression was detected with the Anti-Xpress™ antibody after 5 minutes of exposure (FIG 9A). Doublets can be seen in the four of the five samples expected to express Wasabi-αENaC lanes in Figure 9A (lanes 4-8), likely due to varying glycosylation. The nitrocellulose membrane was then stripped of antibodies, and probed again with the anti-αENaC antibody and imaged after 1 minute of exposure (FIG 9B). Also, the lacZ protein was not reactive with the Anti-αENaC antibody due to the specificity of the anti-αENaC antibody (FIG 9B). The signal was too strong to make out the individual doublets

that were seen after probing with Anti-Xpress™ (FIG 9A). To ensure that the lysis protocol worked properly the nitrocellulose was probed for a third time with Anti-β-actin antibody (FIG 9C).

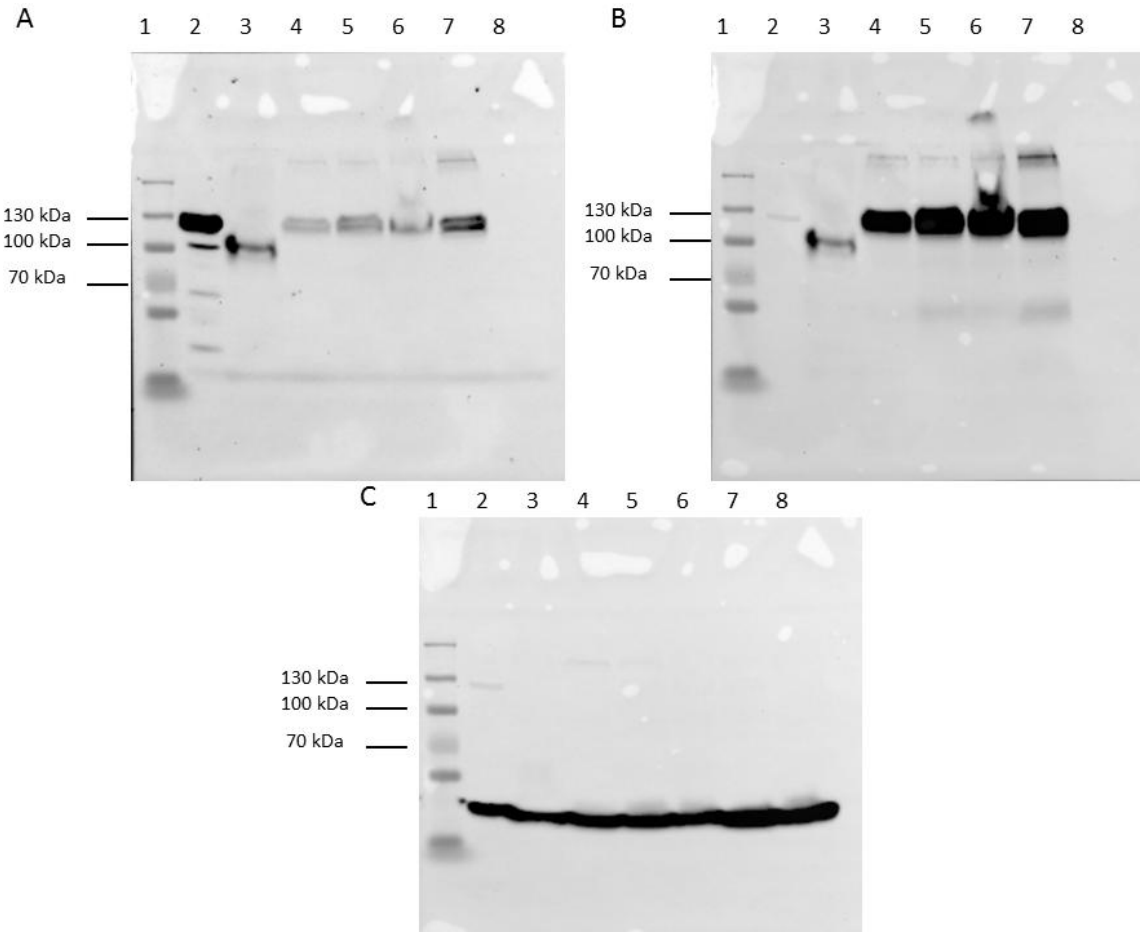

FIG 9. **Western Blots of whole cell lysates from BY4742 and Yeast Deletion strains.** pYES2/NTA/lacZ, pYES2/NTA/αENaC, and pYES2/NTA/Wasabi-αENaC plasmids were transformed into yeast for expression of the Wasabi-αENaC fusion protein. ***A*** – blot probed with Anti-Xpress™ antibody (1:5000 dilution) and ***B*** – blot probed with anti-αENaC antibody (1:1000 dilution). ***C*** – blot probed with anti-β-actin antibody (1:1000 dilution) for lysis protocol control. *lane 1,* PageRuler™ Plus Prestained protein ladder. *lane 2,* lac Z control. *lane 3*, αENaC. *lane 4,* Wasabi-αENaC. *lane 5,* Wasabi-αENaC from *SCJ1* deletion strain. *lane 6,* Wasabi-αENaC from *JEM1* deletion strain. *lane 7,* Wasabi-αENaC from *LHS1* deletion strain. *lane 8,* Wasabi-αENaC from *YPK1* deletion strain.

Dilution "Pronging" Survival Assays

Yeast dilution "pronging" survival assays were carried out to initially screen potential gene deletion candidates to look for differences in growth compared to WT that could be attributed to functional changes in ENaC. Cells were plated on SC-Uracil agar plates using either glucose (to serve as controls) or galactose as the carbon source since galactose induced expression via the *GAL1* promoter (FIG 10).

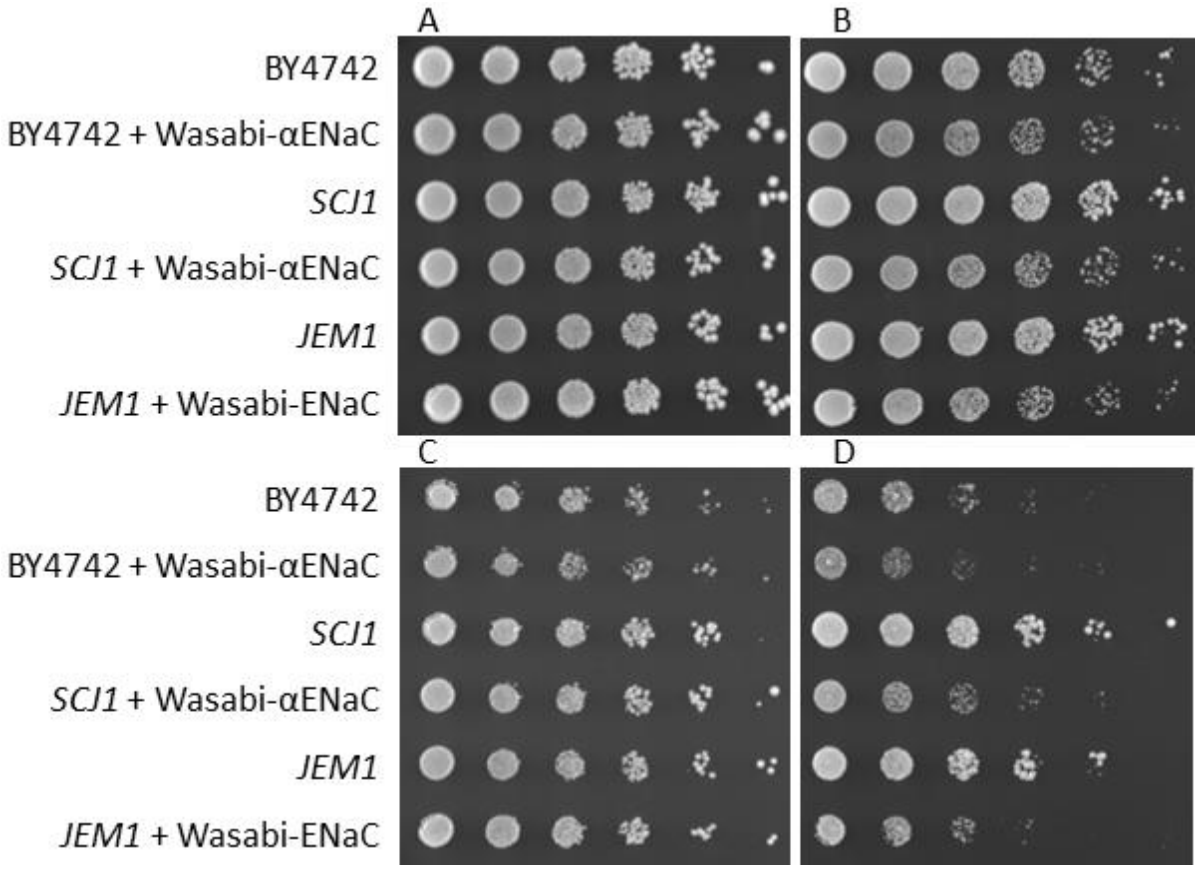

FIG 10. **Survival dilution growth "Pronging" assay of *SCJ1 and JEM1* cells.** pYES2/NTA empty vector and pYES2/NTA/Wasabi-αENaC were transformed into BY4742 yeast as well as *SCJ1* and *JEM1* deletion strains, causing salt-sensitivity and cells were plated to see differences in growth compared to the control. ***A*** - Cells grown on SC-Uracil with 2% glucose. ***B*** - Cells grown on SC-Uracil with 2% galactose. ***C*** - Cells grown on SC-Uracil with 2% glucose and additional 0.75 M NaCl. ***D*** - Cells grown on SC-Uracil with 2% galactose and additional 0.75 M NaCl.

In the presence of excess salt (0.75 M), both scj1 and jem1 cells with Wasabi-αENaC and without Wasabi-αENaC displayed less growth inhibition (i.e., a possible

decrease in ENaC function for the cells transformed with the Wasabi-αENaC genes) compared to the Wasabi-αENaC BY4742 control and the empty vector BY4742 control, respectively (FIG 10D). When compared to the empty pYES2/NTA vector controls, all three strains (BY4742, *SCJ1*, and *JEM1*) did exhibit growth inhibition when expression of ENaC was turned on in the presence of excess salt (FIG 10D). Increased sodium intake due to expression of Wasabi-αENaC, even in minimal salt conditions found in the media, caused modest growth inhibition in the presence of galactose for the three strains (FIG 10B rows 2, 4, and 6). Scj1 and Jem1 are Hsp40 (heat shock protein 40 kDa) chaperone proteins found in the endoplasmic reticulum (ER) lumen and have been shown to prevent aggregation of misfolded proteins and translocate misfolded proteins from the ER to the cytosol for degradation as part of the ER associated degradation (ERAD) pathway (15). Studies by Buck *et al.* show that ERAD of ENaC was inhibited by the simultaneous knockouts of both *scj1* and *jem1,* but the study did not show data regarding the single deletion of each gene (23). We hypothesized that aggregation of misfolded ENaC in the ER could occur when the individual genes were knocked out in the *SCJ1* and *JEM1* deletion strains leading to decreased localization in the cellular membrane and less growth inhibition (attributed to decreased ENaC function) in the presence of excess salt compared to the wild type. The scj1 and jem1 yeast cells with (FIG 10D, Row 4 and 6, respectively) and without (FIG 10D, Row 3 and 5, respectively) expression of Wasabi-αENaC exhibited better growth in excess salt compared to the wild type strain, BY4742, with and without Wasabi-αENaC (FIG 10D, Row 2 and 1, respectively) indicating that knockout of these genes are likely affecting other cellular

processes as well. To further investigate the effect of knockouts on ENaC and its localization, confocal microscopy studies were used to look at Wasabi-αENaC's distribution throughout the cells.

The ypk1 strain without (FIG 11A-D, Row 3) and with (FIG 11A-D, Row 4) Wasabi-αENaC displayed growth inhibition compared to the wild type (FIG 11A-D, Rows 1 and 2) on each type of media and a more pronounced inhibition of growth was seen in the presence of 0.75 M salt (FIG 11D). Ypk1 is the yeast homolog of Sgk1 which, stated earlier, is involved in the upregulation of ENaC in mammalian cells by preventing degradation by Nedd4 so we speculated that the knockout of this protein would lead to down regulation of ENaC, decreasing its function. Decrease in function would then lead to less growth inhibition from less sodium reabsorption with respect to the wild type. This data conflicts, however, in that the overexpression of Wasabi-αENaC in this knockout should cause less growth inhibition of the cells compared to the wild type, but that was not seen (FIG 11). Interestingly, Wasabi-αENaC could not be detected via western blot (FIG 9), but when expression was induced either in the presence or absence of excess salt, there appeared to be a strong inhibition of growth that could be attributed to expression of Wasabi-αENaC (FIG 11B and D, Rows 3 and 4). Since ENaC is not natively found in yeast, it was speculated that Ypk1 must therefore have other ranging effects on overall fitness in yeast and its knockout seemed detrimental.

Growth of lhs1 cells was less inhibited (i.e., decrease in ENaC function) by the excess salt compared to the wild type when expressing Wasabi-αENaC (FIG 11B and D, row 6). As above with scj1 and jem1 cells, lhs1 strains not expressing Wasabi-αENaC

grew better than the control indicating again that other cellular processes were likely being interrupted (FIG 11D, Row 5 and 1, respectively). *Lhs1* is the yeast homolog to GRP170, a Hsp70 (heat shock protein 70 kDa) chaperone protein and is also part of the ERAD pathway (24). As with *SCJ1* and *JEM1*, we hypothesized that *LHS1* yeast expressing Wasabi-αENaC could be forming aggregates of Wasabi-αENaC in the ER, in turn decreasing localization to the cell membrane. To check this and to observe ENaC localization in *YPK1* cells as well, confocal microscopy studies were used to view cell localization.

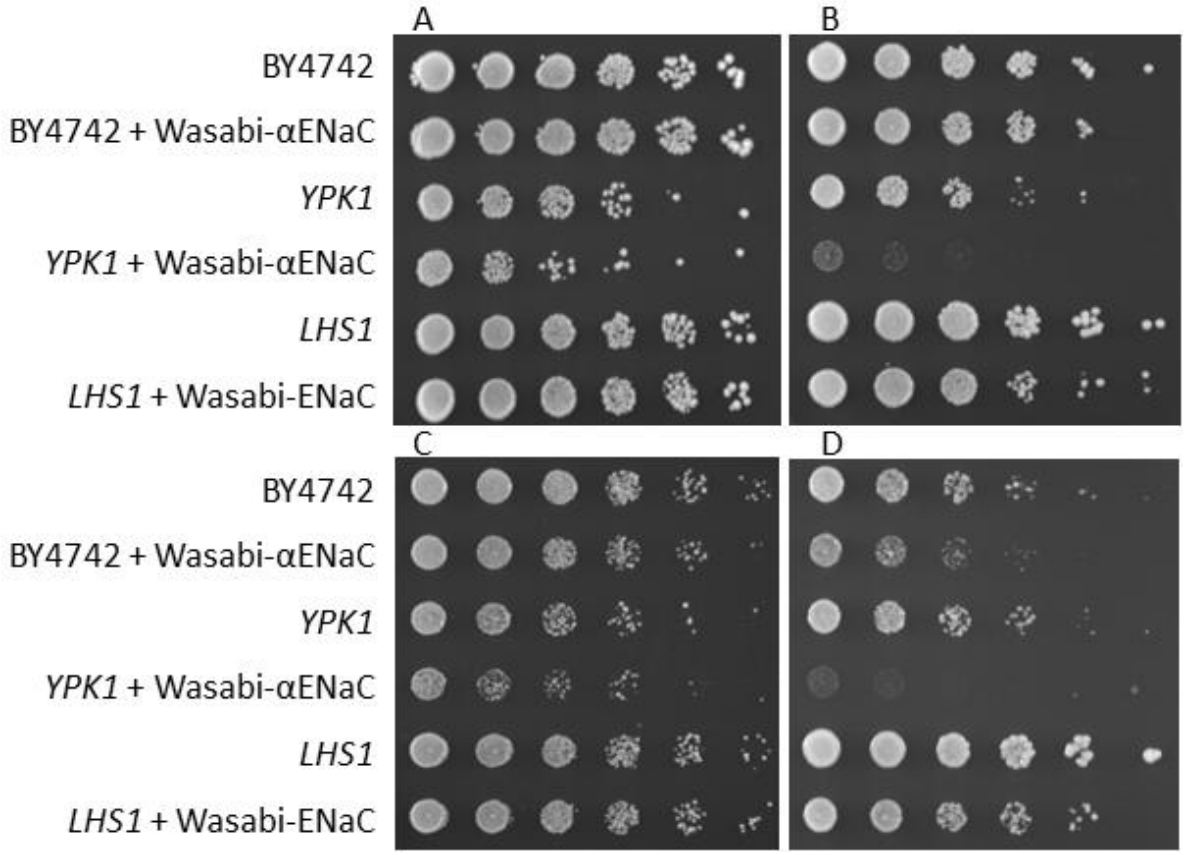

FIG 11. **Survival dilution growth "Pronging" assay of *YPK1* and *LHS1* cells.** pYES2/NTA empty vector and pYES2/NTA/Wasabi-αENaC were transformed into BY4742 yeast as well as *YPK1* and *LHS1* deletion strains, causing salt-sensitivity and cells were plated to see differences in growth compared to the control. ***A*** - Cells grown on SC-Uracil with 2% glucose. ***B*** - Cells grown on SC-Uracil with 2% galactose. ***C*** - Cells grown on SC-Uracil with 2% glucose and additional 0.75 M NaCl. ***D*** - Cells grown on SC-Uracil with 2% galactose and additional 0.75 M NaCl.

Confocal Microscopy and Localization Studies

Confocal microscopy was used to visualize yeast expressing the enhanced green fluorescent protein (EGFP) called Wasabi that was conjugated to αENaC. In addition to cloning pYES2/NTA/Wasabi-αENaC, EYFP-αENaC was cloned from pEYFP-αENaC (also donated from Dr. Jim Stockand) into pYES2/NTA to make the yeast expression vector pYES2/NTA/EYFP-αENaC. A single mutation in the gene for EGFP results in EYFP and changes the fluorescence from green to yellow. Since the gene for EFYP was so similar to Wasabi, the exact same cloning protocol detailed above, including PCR primers and PCR protocol, was followed to clone pYES2/NTA/EYFP-αENaC (data not included). Initial studies indicated that protein expression was higher in yeast transformed with pYES2/NTA/Wasabi-αENaC than in yeast transformed with pYES2/NTA/EYFP-αENaC (data not shown), but the yeast was used in microscopy studies for comparison to yeast expressing Wasabi-αENaC though not used in any pronging assays.

Cells were prepared by inducing expression in 10 mL cultures for 8 hours following the expression protocol above. After pelleting the cells and washing with PBS, the cells were fixed in a 4% v/v formaldehyde/PBS solution, washed again, and resuspended in PBS. The cells were then wet mounted to microscope slides. Cells were viewed using the Olympus FLUOVIEW FV1000 confocal laser scanning microscope with a 60X oil immersion objective and imaged with the accompanying software. Cells expressing Wasabi-αENaC were excited with a laser at a wavelength of 405 nm to visualize the green fluorescence, and cells expressing EYFP-αENaC were excited with a laser at 515 nm to see the yellow fluorescence.

BY4742 cells without the gene for Wasabi-αENaC or EYFP-αENaC did not fluoresce, as expected, and served as the negative control (FIG 12A). The cells expressing Wasabi-αENaC showed even fluorescence throughout the cell membrane while the cells expressing EYFP-αENaC typically fluoresced in pockets around the cell as opposed to the more even fluorescence seen with Wasabi-αENaC (FIG 12D and G).

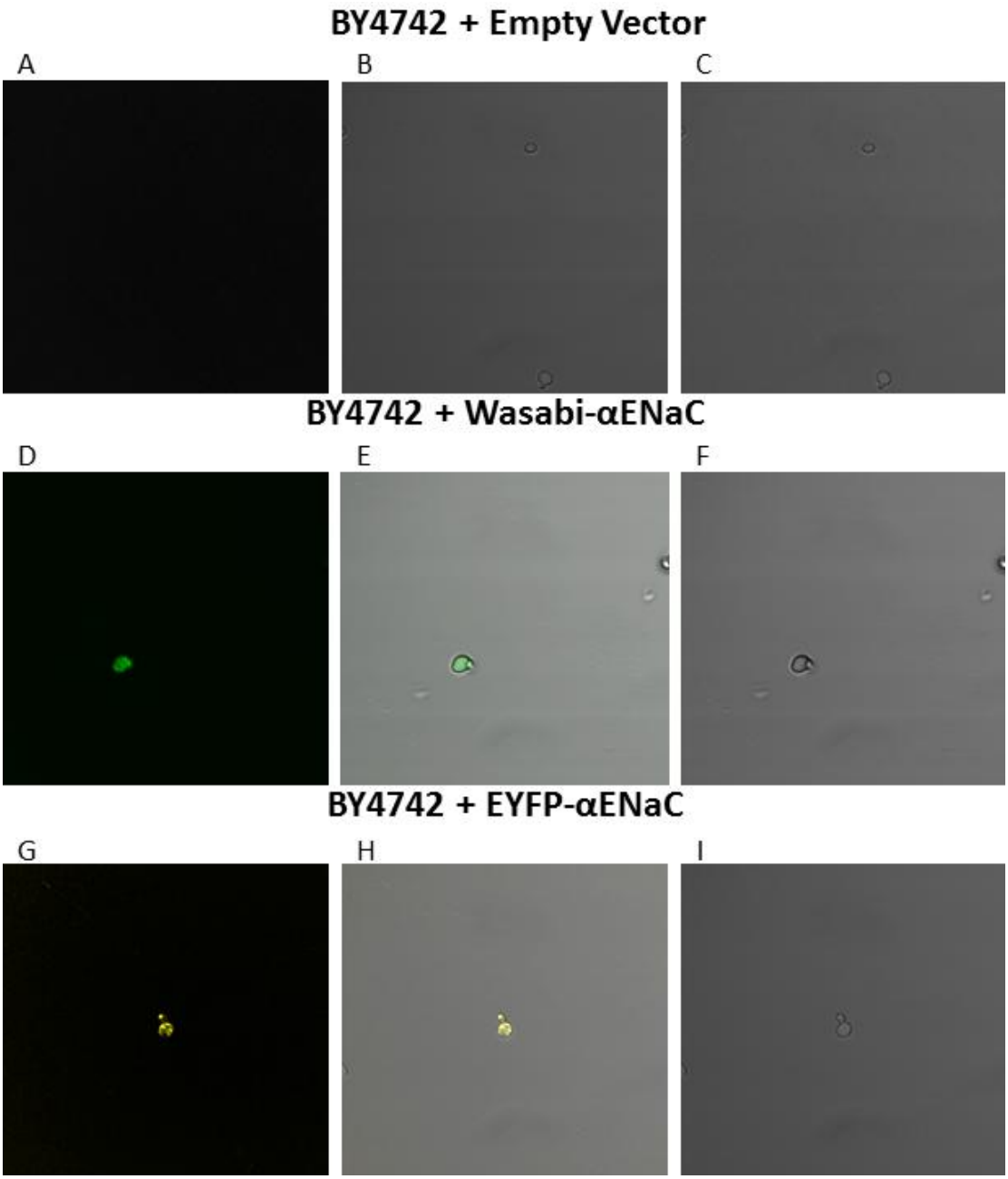

FIG 12. **Confocal microscopy of BY4742 Cells transformed with pYES2/NTA, pYES2/NTA/Wasabi-αENaC, and pYES2/NTA/EYFP-αENaC.** BY4742 yeast cells were transformed with plasmid DNA expressing either Wasabi-αENaC (row 2) or EYFP-αENaC (row 3). The empty vector control (row 1) was used to verify that background fluorescence was not occurring. Column 1 (panels A, D, and G); yeast with GFP or EYFP filter. Column 2 (panels B, E, and H); yeast with GFP or EYFP filter with transmitted light. Column 3 (panels C, F, and I); transmitted light only.

The scj1 cells containing the appropriate plasmid could express both Wasabi-αENaC and EYFP-αENaC (FIG 13A and D). The cells expressing Wasabi-αENaC had an

even distribution of the protein throughout the cell membrane while the protein in cells expressing EYFP-αENaC appeared to be clumped together in the cytosol when viewed under the microscope (FIG 13D-E).

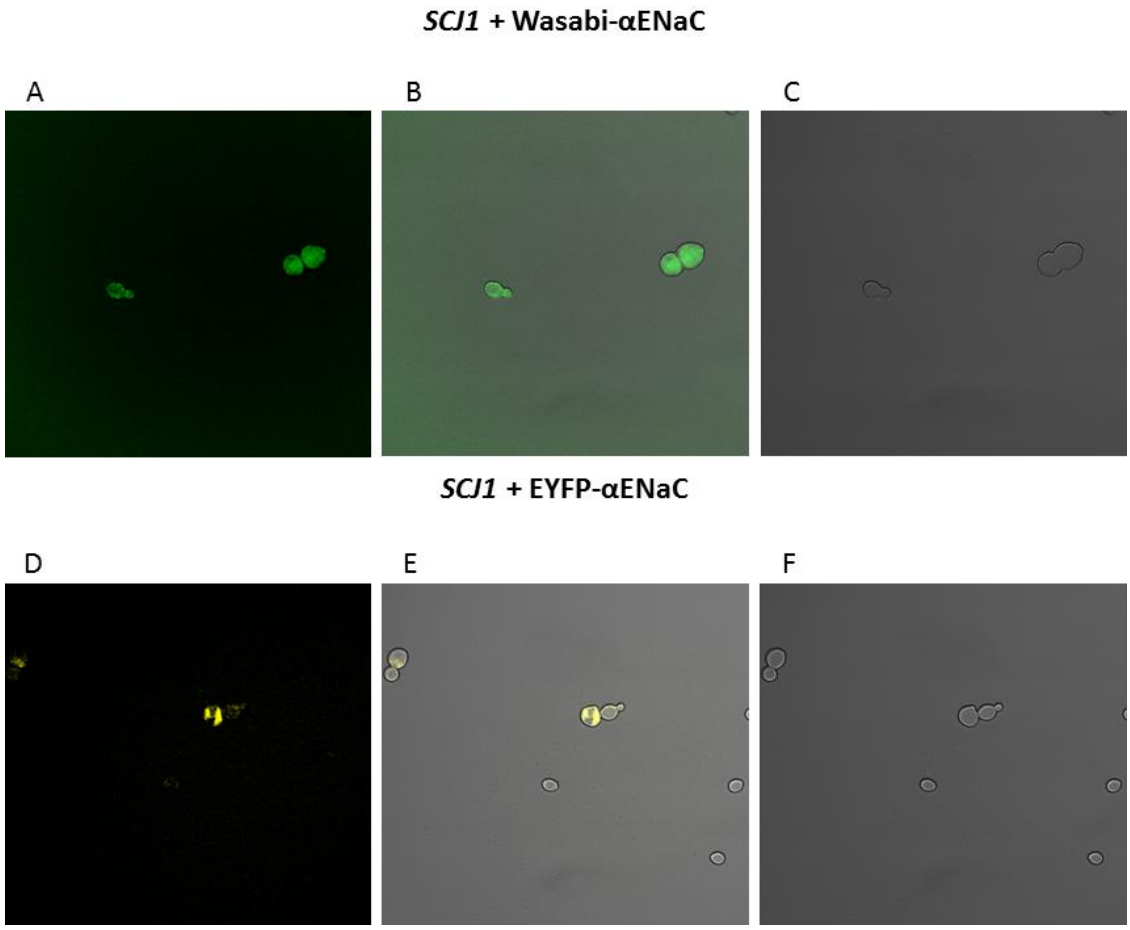

FIG 13. **Confocal microscopy of *SCJ1* cells transformed with pYES2/NTA/Wasabi-αENaC or pYES2/NTA/EYFP-αENaC.** *SCJ1* yeast cells were transformed with plasmid DNA expressing either Wasabi-αENaC (row 1) or EYFP-αENaC (row 2). Column 1 (panels A and D); yeast with GFP or EYFP filter. Column 2 (panels B and E); yeast with GFP or EYFP filter with transmitted light. Column 3 (panels C and F); transmitted light only.

The jem1 cells were also able to express both Wasabi-αENaC and EYFP-αENaC (FIG 14A and D). In this case, however, the fluorescence in both cells seemed to be compartmentalized within the cell as opposed to fluorescing evenly throughout the membrane (FIG 14A-B and D-E). This pattern indicated that the ENaC in these cells do

not localize to the membrane like the wild type and this could be a result of the deletion of the Jem1 protein.

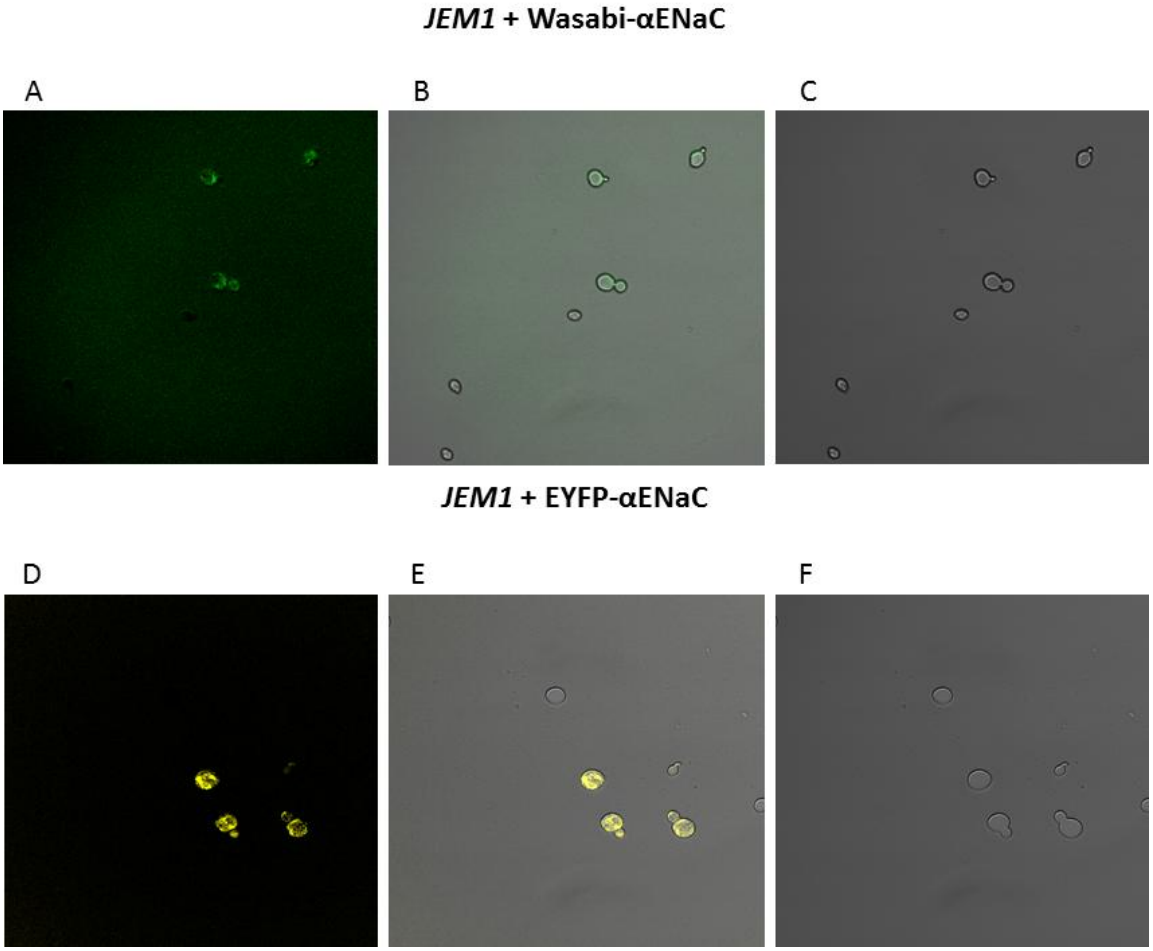

FIG 14. **Confocal microscopy of *JEM1* cells transformed with pYES2/NTA/Wasabi-αENaC or pYES2/NTA/EYFP-αENaC.** *JEM1* yeast cells were transformed with plasmid DNA expressing either Wasabi-αENaC (row 1) or EYFP-αENaC (row 2). Column 1 (panels A and D); yeast with GFP or EYFP filter. Column 2 (panels B and E); yeast with GFP or EYFP filter with transmitted light. Column 3 (panels C and F); transmitted light only.

The ypk1 cells did not express either Wasabi-αENaC or EYFP-αENaC (FIG 15). The lack of expression of the proteins matched what was seen in the western blots (FIG 9A-B, lane 8), but this contradicted what was seen in the pronging assay with *YPK1* cells transformed with pYES2/NTA/Wasabi-αENaC (FIG 11D). Pronging assay results indicated that overexpression of Wasabi-αENaC was occurring in ypk1 cells (FIG 11) and that Ypk1

may function similarly to Sgk1. Since ENaC is not natively found in yeast, it is also likely that Ypk1, though the homolog to mammalian Sgk1, may not function the same way on ENaC as Sgk1 does. Since expression of the protein could never be confirmed in ypk1 cells, that information could not be obtained from this particular study.

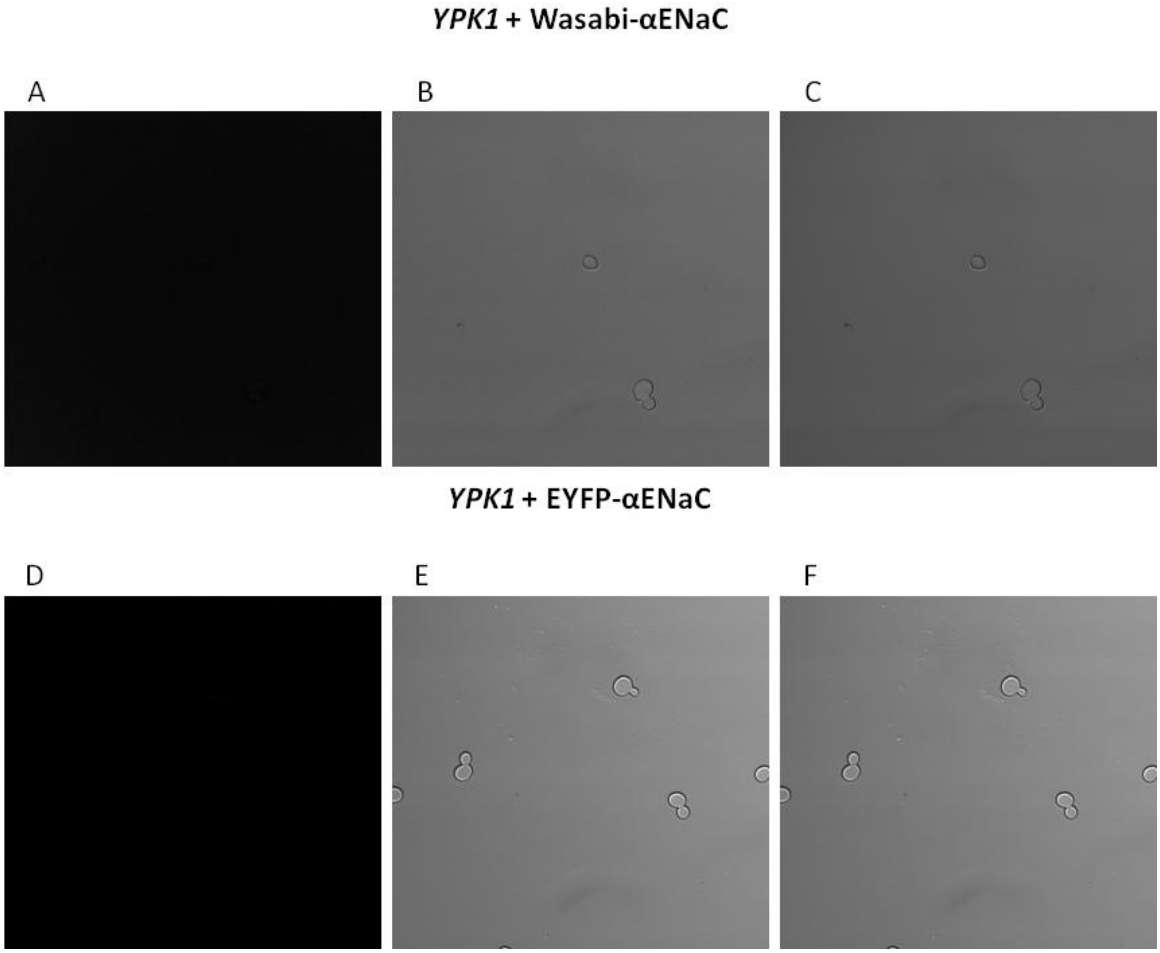

FIG 15. **Confocal microscopy of *YPK1* cells transformed with pYES2/NTA/Wasabi-αENaC or pYES2/NTA/EYFP-αENaC.** *YPK1* yeast cells were transformed with plasmid DNA expressing either Wasabi-αENaC (row 1) or EYFP-αENaC (row 2). Column 1 (panels A and D); yeast with GFP or EYFP filter. Column 2 (panels B and E); yeast with GFP or EYFP filter with transmitted light. Column 3 (panels C and F); transmitted light only.

The *LHS1* cells were able to express both Wasabi-αENaC and EYFP-αENaC and fluoresced when viewed under the microscope (FIG 16A and D). The yeast with EYFP-αENaC showed similar fluorescence as before in that the protein was not being

efficiently inserted into the cell membrane as did the yeast expressing Wasabi-αENaC (FIG 16B and D).

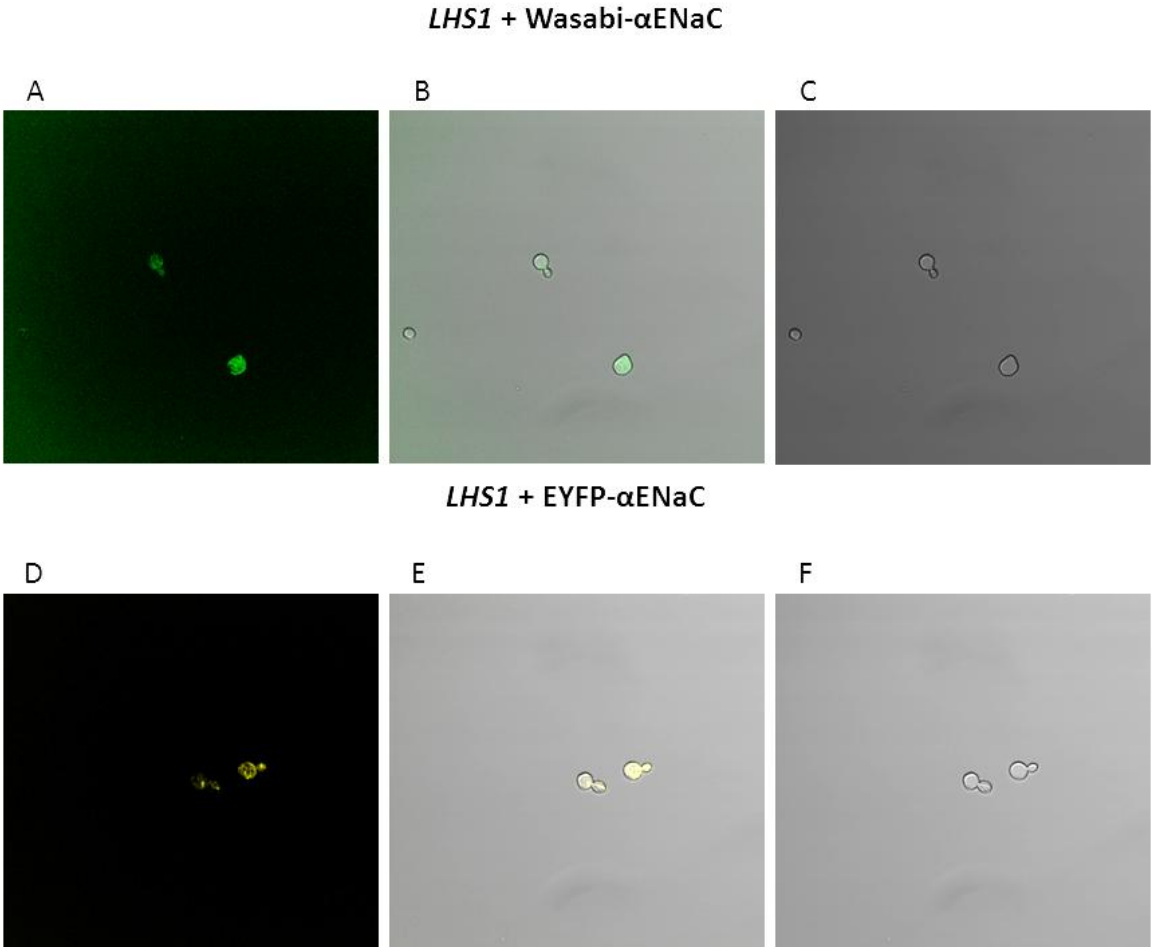

FIG 16. **Confocal microscopy of *LHS1* cells transformed with pYES2/NTA/Wasabi-αENaC or pYES2/NTA/EYFP-αENaC.** *LHS1* yeast cells were transformed with plasmid DNA expressing either Wasabi-αENaC (row 1) or EYFP-αENaC (row 2). Column 1 (panels A and D); yeast with GFP or EYFP filter. Column 2 (panels B and E); yeast with GFP or EYFP filter with transmitted light. Column 3 (panels C and F); transmitted light only.

In summary, with the exception of the *ypk1* strains, all of the yeast cells were able to express the fluorescent Wasabi-αENaC and EYFP-αENaC fusion proteins. Since confirmation of the expression of the fluorescent proteins had been obtained, localization studies could be used to paint a clearer picture of how the translocation of ENaC could be affected by the deletion of the genes coding for the Hsp40 proteins Scj1

and Jem1 as well as the Hsp70 protein Lhs1. There appeared to be something wrong with the EYFP-αENaC fusion protein from a functional standpoint because in each of the 5 strains, the proteins appear to be localizing in the cytosol in vesicles or possibly the ER instead of expressing in the cell membrane. It was decided after this initial confocal study to use only the cells expressing Wasabi-αENaC for the rest of the experiments. To study localization in the cell, Hoechst 33342 was used to stain the nucleus with a fluorophore that would fluoresce with a blue color. By merging those images with that of the green fluorescence images from looking at the Wasabi-αENaC protein, we could hopefully get an idea of where in the cell Wasabi-αENaC was localizing with respect to the nucleus in both wild type BY4742 cells as well as the deletion strains of yeast.

For the localization studies, cells were grown and fixed as mentioned above. After fixation, cells were resuspended in Hoechst 33342 dye, to illuminate the nucleus, that was diluted from 10,000X to 1X in PBS and cells were incubated for 20 minutes at room temperature. After incubation, cells were wet mounted to slides and viewed using the Olympus FLUOVIEW FV1000 confocal laser scanning microscope. Wasabi-αENaC fluorescence was excited by a laser at 415 nm and fluorescence of Hoechst 33342 was excited at 350 nm.

Fluorescence of BY4742 yeast expressing Wasabi-αENaC was observed and it appears that when the image of the Wasabi-αENaC fluorescence was merged with the Hoechst 33342 fluorescence of the nucleus, the Wasabi-αENaC was localizing to the membrane with respect to the nucleus (FIG 17). This was expected since the lack of gene knockouts should allow normal cellular processes to take place and allow for

proper regulation and insertion of Wasabi-αENaC into the membrane. The localization of Wasabi-αENaC in BY4742 cells was used as a reference for the deletion strain localization studies.

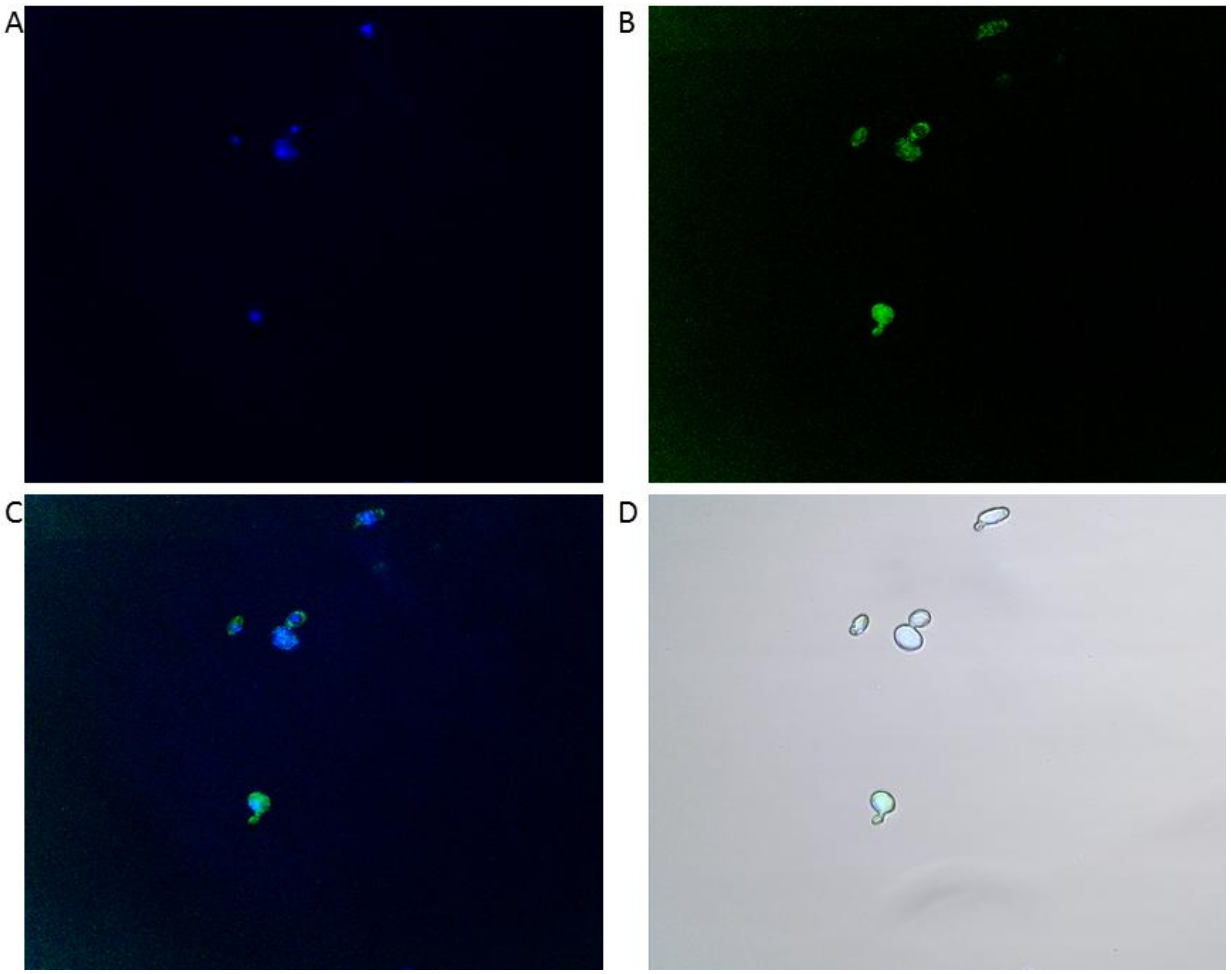

FIG 17. **Co-localization studies of BY4742 cells transformed with pYES2/NTA/Wasabi-αENaC and stained with Hoechst 33342 to illuminate the nucleus.** BY4742 yeast cells were transformed with plasmid DNA expressing Wasabi-αENaC, fixed with a 4% formaldehyde PBS solution, stained with Hoechst 33342 and imaged using confocal microscopy. ***A*** - Yeast imaged using Hoechst 33342 dye filter. ***B*** - Yeast imaged with GFP filter. ***C*** - Panels A and B merged. ***D*** - Hoechst 33342 filter, GFP filter and transmitted light merged.

In scj1 cells expressing Wasabi-αENaC, localization of the protein in the membrane occurred (FIG 18). The fluorescence of Wasabi-αENaC in this study (FIG 18B) was similar to what was seen in the initial confocal studies (FIG 13) indicating that Scj1 is not critical for ENaC function and insertion into the membrane since its deletion did not alter the localization of the protein or alter its function. Although the pronging assay indicated less growth inhibition (decreased ENaC function) compared to the wild type (FIG 9D, Row 4 and 2, respectively), this data was inconclusive since the scj1 control cells not expressing Wasabi-αENaC also grew better than the wild type cells that were not expressing Wasabi-αENaC either (FIG 9D, Row 3 and 1, respectively).

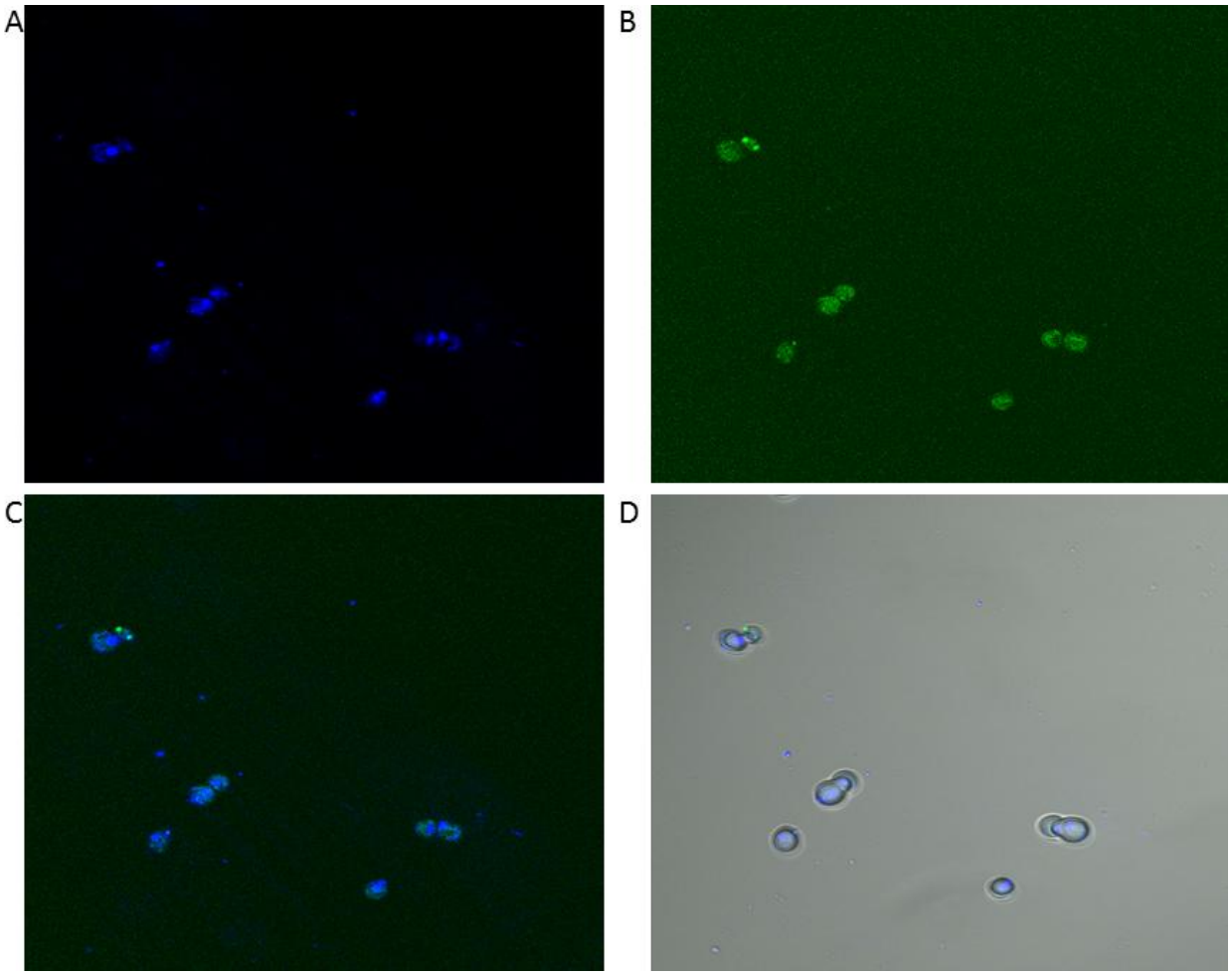

FIG 18. **Co-localization studies of *SCJ1* cells expressing Wasabi-αENaC and stained with Hoechst 33342 to illuminate the nucleus.** *SCJ1* yeast cells expressing Wasabi-αENaC were fixed with a 4% formaldehyde PBS solution stained with Hoechst 33342 and imaged using confocal microscopy. ***A*** - Yeast imaged using Hoechst 33342 dye filter. ***B*** - Yeast imaged with GFP filter. ***C*** - Panels A and B merged. ***D*** - Hoechst 33342 filter, GFP filter and transmitted light merged.

The jem1 yeast expressing ENaC show expression in the membrane, but it also appeared that protein was localizing around the nucleus in the ER when the Wasabi-αENaC fluorescence was merged with the Hoechst 33342 fluorescence (FIG 19C). Though the ER localization was not evident in *JEM1* knockout yeast expressing Wasabi-αENaC the initial study with the confocal microscope (FIG 14), this data corresponds to previous studies which indicate that deletion of the *SCJ1* and *JEM1* genes increased localization of ENaC in the ER (23). Although the pronging assay results are inconclusive

since both the *SCJ1* and *JEM1* empty vector controls grew better than the wild type empty vector control (FIG 10), we speculate that the deletion of *JEM1* causes aggregation of ENaC in the ER and suggest that this protein is critical for regulation of ENaC in the ER. Since deletion of the Scj1 protein did not appear to affect localization (FIG 13), it is also possible the results found by Buck and associates (23) that indicated the double knockout of *scj1* and *jem1* affect ERAD of ENaC could be due to the deletion of *jem1* and not the deletion of *scj1*.

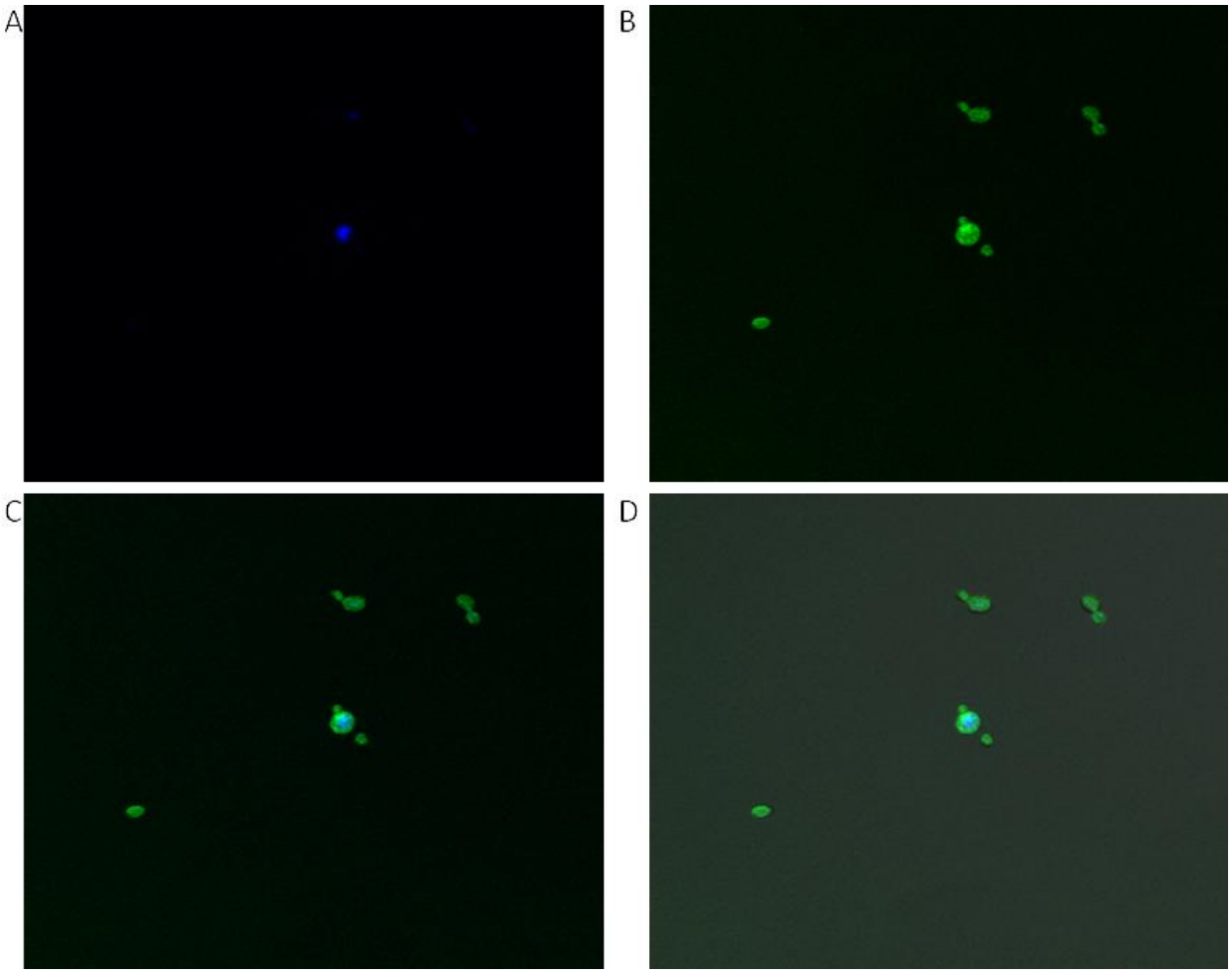

FIG 19. **Co-localization studies of *JEM1* cells expressing Wasabi-αENaC and stained with Hoechst 33342 to illuminate the nucleus.** *JEM1* yeast cells expressing Wasabi-αENaC were fixed with a 4% formaldehyde PBS solution stained with Hoechst 33342 and imaged using confocal microscopy. ***A*** - Yeast imaged using Hoechst 33342 dye filter. ***B*** - Yeast imaged with GFP filter. ***C*** - Panels A and B merged. ***D*** - Hoechst 33342 filter, GFP filter and transmitted light merged.

Again, ypk1 cells did not express Wasabi-αENaC and did not fluoresce when viewed under the microscope though the nucleus was visible from the intercalation and fluorescence of Hoechst 33342 in the nuclear DNA (FIG 20). No expression of Wasabi-αENaC was observed in the western blots or confocal studies, but it did appear that expression of Wasabi-αENaC was occurring in the pronging assay (FIG 11D, Row 6) since inhibition of growth in excess salt occurred when compared to the empty vector control (FIG 11D, Row 5). Sgk1 upregulates ENaC function in mammalian cells so it is believed

that one of two things may be happening with *ypk1* deletion. First, deletion of *YPK1* could be leading to overactive Nedd4 (or the yeast equivalent) which would lead to excessive degradation of ENaC with Nedd4. The other possibility is that Ypk1 is involved in more complex processes in yeast than Sgk1 is in mammalian cells and the deletion of its gene could prevent ENaC expression in yeast as well as other negative effects seen with respect to the fitness of the yeast compared to the BY4742 wild type.

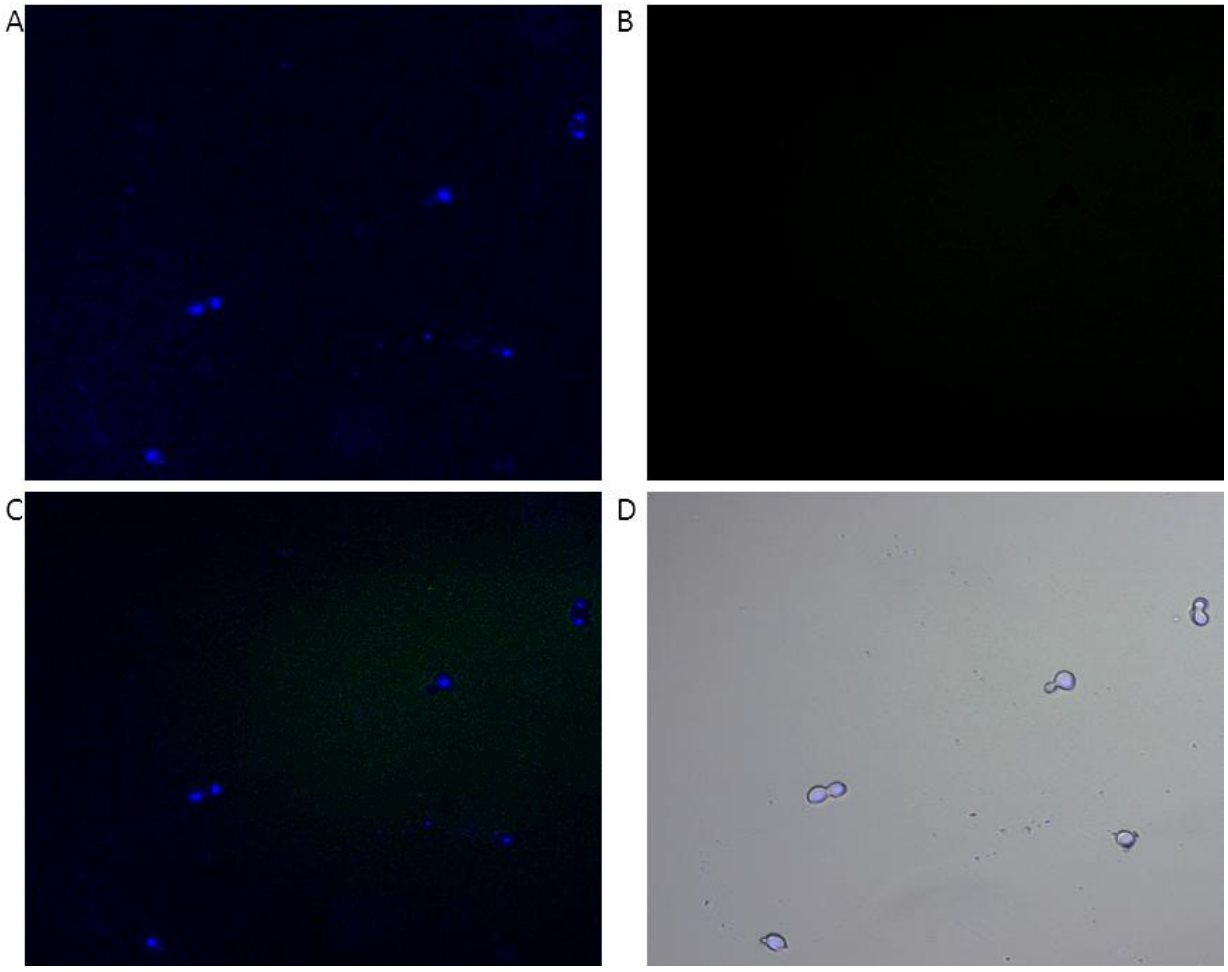

FIG 20. **Co-localization studies of *YPK1* cells expressing Wasabi-αENaC and stained with Hoechst 33342 to illuminate the nucleus.** *YPK1* yeast cells expressing Wasabi-αENaC were fixed with a 4% formaldehyde PBS solution stained with Hoechst 33342 and imaged using confocal microscopy. ***A*** - Yeast imaged using Hoechst 33342 dye filter. ***B*** - Yeast imaged with GFP filter. ***C*** - Panels A and B merged. ***D*** - Hoechst 33342 filter, GFP filter and transmitted light merged.

The Wasabi-αENaC fluorescence in *LHS1* cells (FIG 21) appears blotchy compared to the wild type (FIG 17) and does not appear to be pooling around the nucleus so it looks as though the Wasabi-αENaC protein is pooling in vesicles in the cytosol which correlates to the initial confocal studies (FIG 16) . Lhs1, as reported earlier, is part of the ERAD pathway so it was believed that deletion of its gene would lead to increased localization in the ER compared to the plasma membrane. We saw that localization in

the membrane was reduced with deletion of the *lhs1* gene and believe that Lhs1 is critical for proper ENaC function and insertion into the plasma membrane, but further studies should be carried out to confirm this.

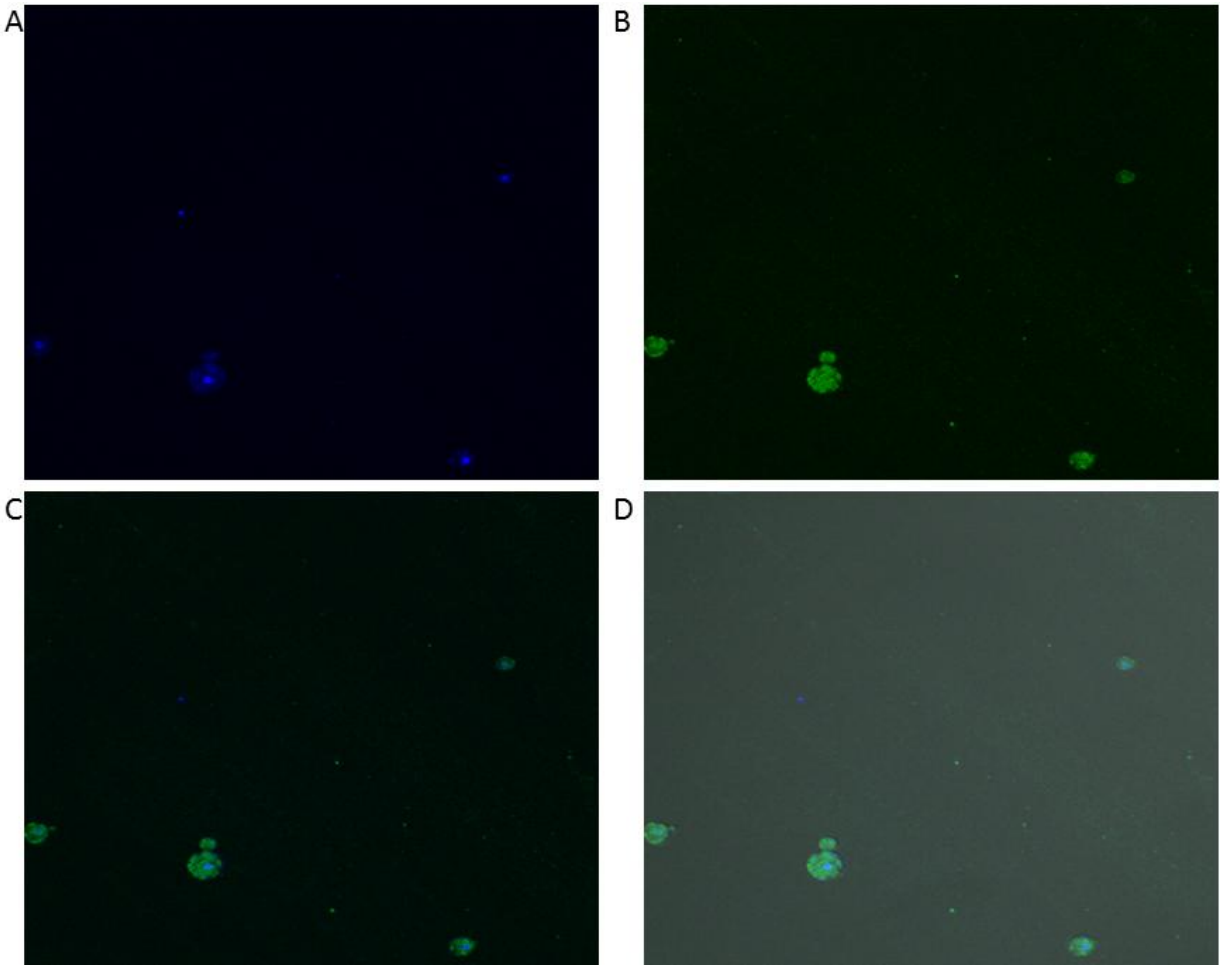

FIG 21. **Co-localization studies of *LHS1* cells expressing Wasabi-αENaC and stained with Hoechst 33342 to illuminate the nucleus.** *LHS1* yeast cells expressing Wasabi-αENaC were fixed with a 4% formaldehyde PBS solution stained with Hoechst 33342 and imaged using confocal microscopy. ***A*** - Yeast imaged using Hoechst 33342 dye filter. ***B*** - Yeast imaged with GFP filter. ***C*** - Panels A and B merged. ***D*** - Hoechst 33342 filter, GFP filter and transmitted light merged.

Conclusions and Future Work By cloning Wasabi-αENaC into a yeast expression vector, we were able to use confocal microscopy and fluorescence to monitor cellular localization of ENaC in yeast deletion strains that have genes thought to be critical for proper ENaC function deleted. Deletion of the *SCJ1* gene did not appear to have any

effects on ENaC function or localization. Jem1 appears to be a protein critical for regulation of misfolded ENaC and translocation of these misfolded proteins to the cytosol for degradation. Data for *ypk1* deletion is inconclusive since expression of the Wasabi-αENaC protein could never be verified although the yeast appears salt sensitive after transformation of the Wasabi-αENaC gene. As noted earlier, Ypk1 was shown, in yeast, to affect cell wall integrity when the gene for Ypk1 was knocked out. It is possible that the cell walls are not as strong which could lead to sodium entering the cell through a porous membrane even though ENaC presence could not be detected. Finally, we report that *LHS1* deletion leads to decreased localization in the membrane and increased localization in the cytosol, likely due to aggregation of ENaC in the ER although ER localization is not entirely clear from the data. In conclusion, a functioning Wasabi-αENaC fusion protein was created and can be used to study the effects of accessory protein knockouts on cellular localization in yeast. This can further elucidate the regulatory pathway for insertion of ENaC into the plasma membrane and help ENaC researchers understand the role of different accessory proteins on ENaC function.

Future studies include using cell surface biotinylation to quantify the amount of Wasabi-ENaC being localized in the membrane compared to the cytosol in the deletion strains of yeast where membrane localization does not seem to be occurring. Also, confocal fluorescence studies can be used with ER, Golgi, and plasma membrane antibodies conjugated with fluorophores so that further elucidation of ENaC localization can be worked out with more extensive co-localization studies. With regard to the ypk1 strain, one future study that can be carried out to determine if the cell can produce

ENaC is to use the compound MG132 to block degradation. MG132 has been shown in mammalian cells to inhibit proteosomal degradation of ubiquitinated proteins (25). Since the deletion of *YPK1* could lead to over activity of Nedd4 (or its yeast equivalent) and therefore ENaC protein degradation by ubiquitination, blocking this degradation pathway could allow for expression of Wasabi-ENaC to be seen in ypk1 cells if they can, in fact, express the protein. One final suggestion for a future study is to use co-immunoprecipitation to try and precipitate some of the accessory proteins in this study, knocked out in deletion strains, from the BY4742 wild type yeast to see if protein-protein interactions can be observed between ENaC and the accessory proteins.

LITERATURE CITED

1. http://www.cdc.gov/dhdsp/data_statistics/fact_sheets/fs_bloodpressure.htm
2. **Bugaj, V., Mironova, E., Kohan, D. E., and Stockand, J. D.** Collecting duct-specific endothelin B receptor knockout increases ENaC activity. *Am. J. Physiol. Cell Physiol.* 302: C188-C194, 2012
3. **Schild, L.** The epithelial sodium channel and the control of sodium balance. *Biochim. Biophys. Acta.* 1802: 1159-1165, 2010.
4. **Hamm, L. L., Feng, Z., and Hering-Smith, K. S.** Regulation of sodium transport by ENaC in the kidney. *Curr. Opin. Nephrol. Hypertens.* 19: 98-105, 2010.
5. **Canessa, C. M., Horsiberger, J., and Rossier, B. C**. Epithelial sodium channel related to proteins involved in neurodegeneration. *Nature* **361,** 467-470, 1993.
6. **Staruschenko, A., Adams, E., Booth, R. E., and Stockand, J. D.** Epithelial Na^+ Channel Subunit Stoichiometry. *Biophys. J.* 88: 3966-3975, 2005.
7. **Bonny, O. and Hummler, E.** Dysfunction of epithelial sodium transport: From human to mouse. *Kidney Int.* 57: 1313-1318, 2000.
8. **Snyder, P. M.** The Epithelial Na^+ Channel: Cell Surface Insertion and Retrieval in Na^+ Homeostasis and Hypertension. *Endocr. Rev.* 23: 258-275, 2002.
9. **Stockand, J. D., Starushcnko, A., Pochynyuk, O., Booth, R. E., and Silverthorn, D. U.** Insight Toward Epithelial Na^+ Channel Mechanism Revealed by the Acid-sensing Ion Channel 1 Structure. *IUBMB Life* 60: 620-628, 2008.
10. **Jasti, J.,Furukawa, H., Gonzales, E. B., and Gouaux, E**. *Structure of acid-sensing ion channel 1 at 1.9 Å resolution and low pH*. *Nature* 449: 316-323, 2007.
11. **Garty, H. and Palmer, L.G.** *Epithelial sodium channels: function, structure, and regulation*. *Physiol. Rev.* 77(2): 359-396, 1997.
12. **Bankir, L, Bichet, D. G., and Bouby, N**. *Vasopressin V2 receptors, ENaC, and sodium reabsorption: a risk factor for hypertension? Am. J. Renal Physiol.* 299: F917-F928, 2010.
13. **Hendron, E., Patel, P., Hausenfluke, M., Gamper, N., Shapiro, M. S., Booth R. E., and Stockand, J. D.** Identification of Cytoplasmic Domains within the Epithelial Na^+ Channel Reactive at the Plasma Membrane. *J. Biol. Chem.* 277: 34480-34488, 2002.
14. **Snyder, P. M., Olson, D. R., Kabra, R., Zhou, R., and Steines, J. C.** cAMP and Serum and Glucocorticoid-Inducible Kinase (SGK) Regulate the Epithelial Na^+ Channel through Convergent Phosphorylation of Nedd4-2. *J. Biol. Chem.* 279: 45753-45758, 2004.

15. **Qiu, X. B., Shao, Y. M., Miao, S., and Wang, L.** The diversity of the DnaJ/Hsp40 family, the crucial partners for Hsp70 chaperones. *Cell. Mol. Life Sci.* 63: 2560-2570, 2006.
16. **Roelants, F. M., Torrance, P. D., Bezman, N., and Thorner, J.** Pkh1 and Pkh2 differentially phosphorylate and activate Ypk1 and Ykr2 and define protein kinase modules required for maintenance of cell wall integrity. *Mol. Biol. Cell* 9: 3005-3028, 2002.
17. **Craven, R. A., Egerton, M., and Stirling, C. J.** A novel Hsp70 of the yeast ER lumen is required for the efficient translocation of a number of protein precursors. *EMBO J.* 11: 2640-2650, 1996.
18. **Kushnirov, V. V.** Rapid and reliable protein extraction from yeast. *Yeast* 16: 857-860, 2000.
19. http://www.ncbi.nlm.nih.gov/nuccore/257796260
20. http://allele.allelebiotech.com/shopcart/files/products/pmWasabi-N.htm
21. http://www.lifetechnologies.com/order/catalog/product/V825220
22. **Ybanez, R**. 2009. The Development of a Quick Screen in Yeast for Functional Epithelial Sodium Channels. *M.S. Thesis*
23. **Buck, T. M., Kolb, A. R., Boyd, C. R., Kleyman, T. R., and Brodsky, J. L.** The Endoplasmic Reticulum-associated Degradation of the Epithelial Sodium Channel Requires a Unique Complement of Molecular Chaperones. *Mol. Biol. Cell* 21: 1047-1058, 2010.
24. **Buck, T. M., Plavchak, L., Roy, A., Donnelly, B. F., Kashlan, O. B., Kleyman, T. R., Subramanya, A. R., and Brodsky, J. L.** The Lhs1/GRP170 Chaperones Facilitate the Endoplasmic Reticulum-associated Degradation of the Epithelial Sodium Channel. *J. Biol. Chem.* 288: 18366-18380, 2013.
25. **Liu, C., Apodaca, J., Davis, L. E., and Rao, H.** Proteasome inhibition in wild-typeyeast *Saccharomyces cerevisiae* cells. *BIOTECHNIQUES*. 42: 158-162, 2007.